NUTRIENT SENSING MECHANISMS

IN THE

SMALL INTESTINE:

Localisation of taste molecules in mice and

humans with and without diabetes

Kate Sutherland, B.Sc. (Hons)

A thesis submitted in fulfilment of the Degree of Doctor of Philosophy

Discipline of Physiology

School of Molecular and Biomedical Sciences

Adelaide University

October 2008

5. EXPRESSION LEVELS OF TASTE MOLECULES IN THE MOUSE INTESTINAL MUCOSA ARE ALTERED WITH NUTRITIONAL STATE

5.1 Summary

Background: The slowing of gastric emptying in response to intestinal glucose is attenuated after short-term dietary glucose supplementation and exaggerated following starvation. These observations suggest that adaptation occurs in small intestinal mechanisms governing gastric emptying in response to dietary cues. Such adaptation may result from alterations in nutrient detection and signalling molecules in the epithelium and/or corresponding receptors on vagal afferent nerves. *Aims:* To quantify and compare between fed and fasted mice expression of taste transduction molecules and precursors to 5-HT and GLP-1 in intestinal mucosa, and receptors for 5-HT and GLP-1 in vagal afferents. *Methods:* C57 mice were housed in two groups of six, one group was fasted while the other had access a nutrient-rich diet, both for 16-hours. RNA was extracted from the jejunal mucosa and real time RT-PCR used to quantify expression levels for taste molecules, T1R2, T1R3, Gα_{gust} and TRPM5, and both tryptophan hydroxylase-1 (Tph-1) and proglucagon (Gcg). In a similar manner, RT-PCR was performed in nodose ganglia for 5-HT$_3$R and GLP-1R. Expression levels of each target were compared between samples from fed or fasted mice. *Results:* Relative expression data showed that T1R2, T1R3, Gα_{gust} and TRPM5 transcripts were significantly higher in the mucosa of fasted compared to fed mice (n = 6, p < 0.001). Tph-1 was a low abundance transcript in jejunal mucosa but was significantly higher in fasted compared to fed mice (p < 0.0001). Gcg expression did not differ between mouse groups. 5-HT$_3$R transcripts in nodose ganglion were significantly lower in fasted compared to fed mice (p < 0.001). In contrast, GLP-1R transcript levels were significantly higher in the nodose ganglion of fasted mice (p < 0.01). *Conclusions:* Short-term dietary interventions alter the

expression of sweet taste molecules in the jejunal mucosa in mice, suggesting taste cells in the epithelium are able to rapidly adapt to their luminal environment. Changes in the expression of epithelial taste molecules as well as receptor expression in vagal afferents may underlie adaptations in gastrointestinal regulatory mechanisms cause by prior nutrient intake patterns.

5.2 Introduction

It is well established that intestinal nutrients slow gastric emptying via reflexes initiated through receptors in the small intestine (86, 218, 224, 307, 315). Studies in the preceding chapters have confirmed that key components of the lingual sweet taste transduction mechanism are specifically expressed in the small intestinal epithelium and thereby constitute a putative molecular mechanism for detection of intestinal carbohydrates. Furthermore, a population of intestinal 'taste' cells were shown to co-express 5-HT and GLP-1, factors released in response to the presence of carbohydrate in the small intestine that act to slow gastric emptying. Together these findings provide evidence of a potential mechanism whereby intestinal carbohydrates trigger vagal feedback to alter gastric motor function.

The intestinal mechanisms that regulate gastric emptying have been shown to adapt to previous patterns of nutrient intake. For example, a nutrient supplemented diet of either high carbohydrate (63, 143, 271), fat (62) or protein (322) maintained for a period of three to fourteen days significantly accelerated the rate of gastric emptying to the supplemented macronutrient in subsequent meals. This change in gastric emptying did not occur in non-supplemented control diets in both rodents and humans. Conversely, after short-term starvation (four days) gastric emptying was shown to be slowed following glucose intake (57). The rate of gastric emptying is also slower in patients with anorexia nervosa (79, 139), and in these patients can be nomalised with a short-term re-feeding programme (281). The observation that altered feedback occurs only

in response to the specific macronutrient class increased in dietary intake (63) suggests that there is a specific adaptation in the individual mechanisms that detect that nutrient class.

There is limited information on nutrient sensing mechanisms in the small intestine and therefore specific adaptations that underlie altered gastric emptying responses to macronutrients are not clear. Changes in nutrient feedback could reflect alteration in the length of intestinal nutrient exposure (due to numbers of absorptive transporters), or may result from changes in the ability of taste cells to express nutrient receptors or to release vagal neurotransmitters. In addition, altered nutrient feedback may result from altered sensitivity of vagal afferent fibres due to change in the expression of specific receptors expressed on afferent endings.

Both 5-HT and GLP-1 are released from the epithelium in response to intestinal carbohydrates and are key mediators of subsequent feedback processes. The incretin peptide GLP-1 plays a well documented role as a satiating factor as well as in vagally-mediated slowing of gastric emptying (148, 155). 5-HT mediates carbohydrate-induced inhibition of gastric emptying through 5-HT_3 receptors on vagal afferents (269). 5-HT_3R antagonists additionally reduce the satiating effects of intestinal carbohydrates (301) thus also implicating 5-HT in the reduction of food intake in response to intestinal carbohydrates.

5-HT and GLP-1 are expressed in separate populations of enteroendocrine cells with differing distributions along the gastrointestinal tract, namely a more predominant distal location of GLP-1-secreting L cells (345). 5-HT and GLP-1 signalling pathways may be more nutrient or region specific than previously known or these signalling pathways may overlap in function. Recently it has been demonstrated that intestinal nutrient driven satiety is more surmountable when signalling pathways for both CCK and 5-HT are intact than through either pathway when the other receptor type is blocked (302). Similarly GLP-1 and 5-HT signalling mechanisms may act in parallel as well as in an interdependent manner with interactions between pathways

potentially occurring at multiple levels to precisely control functions according to nutritional cues, although this has yet to be directly investigated.

Enterochromaffin cells synthesise 5-HT from tryptophan via pathways catalysed by tryptophan hydroxylase-1 (Tph-1) (105). As the rate-limiting step in this biosynthetic pathway, Tph-1 is considered a marker of 5-HT synthesis. GLP-1, a product of the mammalian proglucagon gene, is formed by post-translational processing of proglucagon by the action of prohormone convertase 1/3 in L-cells of the small intestine (197). Nutrients, particularly fat and peptides, have been shown to alter proglucagon mRNA levels in rat small intestine (56, 151), suggesting that synthesis of gut peptides may be directly regulated by nutrient exposure. Enteroendocrine cell numbers themselves and proportions of enteroendocrine cell subtypes may also change in response to physiological stimuli as new cells rapidly emerge from the crypt and transit to the villus epithelium (282).

Similarly there is evidence that expression levels of some receptors in vagal neurons are up- or down-regulated depending on short-term dietary status (35). The 5-HT subtype 3 (5-HT$_3$) and GLP-1 receptors expressed by vagal neurons receptors (243, 269) may therefore be regulated by prior dietary state and changes at the level of vagal afferents themselves may subserve altered gastrointestinal reflexes to the presence of carbohydrate.

This study aimed to determine whether expression of intestinal taste and/or signalling molecules and their receptors are regulated by dietary status secondary to acute overnight feeding or fasting. This timeframe allows changes to be assessed before epithelial cell renewel (2-3 days) avoided changes resulting from reprogramming of epithelial cell phenotypes and/or from changes in absorptive capacity following longer term dietary interventions.

5.3 Aims

To determine if expression of sweet taste and/or signalling molecules in the intestinal mucosa and corresponding receptors in vagal neurons are altered following short-term dietary intervention.

5.4 Specific hypotheses

1. Expression levels of taste molecules, T1R2, T1R3, $G\alpha_{gust}$ and TRPM5 differ in the intestinal mucosa according to nutritional state in fed and fasted mice.

2. Expression levels of Tph-1 and proglucagon in the intestinal mucosa will differ according to nutritional state in fed and fasted mice.

3. Expression levels of 5-HT$_3$R and GLP-1R in the nodose ganglion will differ according to nutritional state in fed and fasted mice.

5.5 Materials and methods

All experiments were performed using adult male C57BL/6 mice aged 7-10 weeks, housed conventionally with free access to water and a standard laboratory rodent diet. All studies were performed in accordance with the Australian code of practice for the care and use of animals for scientific purposes and with the approval of the Animal Ethics Committees of the Institute of Medical & Veterinary Science (Adelaide, Australia) and the University of Adelaide.

5.5.1 Fed and fasted animals and tissue collection

Twelve adult male C57BL/6 mice were housed as two separate groups of six. One group was fasted over night with no access to food or edible material but with free access to water. The second group was housed with free access to standard laboratory rodent chow enriched with sunflower seeds, peanut butter and honey to promote consumption of high levels of protein, fat and carbohydrate. The food was eagerly consumed by the fed group of mice and only minimal amounts remained at the end of the overnight period. After 16 hrs mice from both groups were killed via CO_2 asphyxiation and tissues dissected in ice-cold sterile saline. The left and right nodose ganglia of each mouse were removed and transferred immediately into RNA stabilisation reagent, RNAlater® (Qiagen, Australia); the nodose ganglia were separated into fed and fasted groups. The jejunum was opened longitudinally; the mucosa removed from muscular layers by scraping using an angled scalpel blade, transferred to a sterile collection tube and snap frozen in liquid nitrogen. At the time of tissue dissection it was noted that stomachs of fasted mice were empty whereas fed mice had full stomachs, confirming their food intake.

5.5.2 RNA extraction

Mucosa

Mucosal samples were disrupted using a glass mortar and pestle without being allowed to thaw. Total RNA was isolated from the mucosa using the RNeasy Mini Kit (Qiagen), as per the manufacturer's instructions for purification of total RNA from animal tissues, including an on-column DNase digestion step (described in detail in Chapter Two). Mucosal RNA was extracted from individual samples then purified RNA from all the fed or fasted mice was separately pooled. The concentration and purity of the final RNA sample was

assessed by UV spectroscopy as described in Chapter Two. The purified template RNA was stored in aliquots of 5 μL at -80°C until use.

Nodose ganglia

Nodose ganglia were pooled into separate fed and fasted samples for RNA extraction. These tissues were transferred into a glass mortar and pestle and TRIzol reagent (Invitrogen, Australia), containing denaturants and RNase inhibitors, was added (total volume 1 ml). The tissue was disrupted and mechanically homogenised in TRIzol reagent using a mortal and pestle. The resulting lysate was then transferred into a QIAshredder spin column in a 2 ml collection tube (Qiagen) to complete homogenisation via centrifugation at 1300 rpm at room temperature for two minutes. The collection tubes containing the homogenate were capped and mixed via vortex and left to stand at room temperature for 15 min. Separation of the homogenate into organic and aqueous phases was achieved by vortex mixing the homogenate with 200 μl of chloroform followed by cold centrifugation at 13000 rpm for 15 min. The upper aqueous phase (containing RNA) was removed by pipette and transferred into a fresh sterile eppendorf. RNA was precipitated out of solution with the addition of 500 μl of isopropanol, mixed by vortex and incubated for 10 min at room temperature. After cold centrifugation (1300 rpm for 10 min) the supernatant was removed and discarded. The pellet was then washed with 1 ml of 75% ethanol via vortex mixing. The tube was then centrifuged for 5 min at 1300 rpm and the supernatant again removed and discarded. RNA was solubilised and resuspended in 100 μl of RNase-free water by pipette mixing and heating at 60ºC for 2 min. The concentration and purity of the resulting RNA sample was assessed by UV spectroscopy and stored in aliquots of 5 μl at -80°C until use.

5.5.3 Primers

Primers used for detection of T1R2, T1R3, Gα_{gust} and TRPM5 genes are detailed in Chapter Two.
Additional primers to specifically detect mouse tryptophan hydroxylase 1 (Tph1), proglucagon (Gcg),
5-HT$_3$R and GLP-1R genes were purchased commercially as validated QuantiTect primer assays (Qiagen).
Details of additional primers are provided in Table 5.5.3 and the gene locations from which detected
transcripts are amplified are shown in Figure 5.5.1.

Table 5.5.3 Primers for amplification of additional mouse genes in real time RT-PCR reactions

Gene	Entrez gene ID	Accession no.	Length of transcript (bp)	Primer information	Amplicon length (bp)
Tph1	21990	NM_009414	2047	QT00152565	124
Gcg	1426	NM_008100	1091	QT00124033	94
5-HT$_3$R (Htr3a)	15561	NM_013561	2071	QT01039885	148
GLP-1R	14652	NM_021332	1480	QT00130767	128

QT, QuantiTect primer assay, catalogue number (Qiagen)

NOTE:
These figures are included on page 187 of the print copy of the thesis held in the University of Adelaide Library.

Figure 5.5.1 Approximate location of amplicon sequences detected by QuantiTect Primer Assays in additional target mouse genes.
In Chapter two taste molecules and reference genes were amplified in PCR reactions using validated forward and reverse primers for specific gene sequences commercially available from Qiagen. Specific sequence information of these commercially available primers and their corresponding amplicons are not available. Schematic representations of the approximate amplified regions of additional target genes used in these studies are shown for tryptophan hydroxylase 1 (Tph1) (A), glucagon (Gcg) (B), 5-HT$_3$R (C) and GLP-1R (D). Schematic representations of taste molecule and reference genes are shown in Chapter two.

5.5.4 Real time RT-PCR protocol

Real time RT-PCR was performed as detailed in Chapter Two using the QuantiTect® SYBR® Green RT-PCR kit (Qiagen) in a one-step RT-PCR protocol according to the manufacturer's instructions. No template control (NT) reactions were constructed by substituting RNA with nuclease-free water. Additional no reverse transcription (-RT) controls were run for T1R3 reactions to correct for any genomic DNA contamination of the sample. Each target and reference assay was run separately, in triplicate, with each RNA sample. Melt curve analyses were used to confirm specificity of the amplified product and some PCR products were further assessed by gel electrophoresis to confirm product size.

5.5.5 Data and statistical analysis

β-actin was chosen as a reference gene as fed and fasted samples in these experiments compared from a single tissue type with preliminary assays confirming β-actin transcript levels did not significantly differ between fed and fasted jejunal samples (results not shown). C_T values for all target and reference reactions were obtained at a threshold of 0.05 as described in Chapter Two. As described for the experiments in Chapter Two, for each reaction, the fluorescence level (R) at time 0 (proportional to initial transcript amount) was calculated by the following formula;

$$R_0 = R_{ct} \times (1 + E)^{-ct}$$

The formula includes a correction for the PCR amplification efficiency (E) of the reaction. Efficiency was calculated by Opticon Monitor software (Biorad) using the real time amplification curve from each reaction to plot a line through the fluorescence level at the C_T and the next two cycles. The slope of this line was the basis for the calculation of PCR efficiency. R_0 was obtained for samples containing target and reference

genes and expressed as the ratio of $R_{0 \text{ target}} / R_{0 \text{ reference}}$ to obtain normalised relative quantification data. In PCR analyses replicate of target and reference reactions were not averaged but treated as independent samples, with each replicate of the target assay expressed as a ratio to each replicate of the reference assay (as described in Chapter 2). Relative RNA levels are expressed as mean ± standard error of the mean (SEM) of all values obtained. Statistical analysis was performed using GraphPad Prism Software (3.02, San Diego, CA) and a Mann-Whitney test was used to compare expression levels of target genes in each tissue type between fed and fasted groups. A p-value of < 0.05 was considered significant.

5.6 Results

5.6.1 Relative expression of taste-signal molecules in jejunal mucosa from fed and fasted mice

Taste molecules T1R2, T1R3, Gα_{gust}, and TRPM5 have been shown to be specifically expressed in the intestinal mucosa of the mouse (Chapter Two). RT-PCR reactions in the current experiments confirmed this taste molecule expression in the jejunal mucosa in both fed and fasted mice groups. Melt curve analyses confirmed the existence of a single PCR product and the absence of primer dimers. The existence of a single PCR product of the predicted size for each primer set was also confirmed by running selected reaction products on an ethidium bromide gel by electrophoresis (Figure 5.6.1) Primer sets generally did not amplify genomic DNA (gDNA) in control reactions with no reverse transcriptase; however, the T1R3 primers did co-amplify gDNA if present in the sample, despite the use of DNase digestion during RNA extraction. In these experiments only mucosal RNA samples from fed mice contained detectable gDNA. The contribution of co-amplified gDNA to the C_T value in these samples was corrected by subtracting the fluorescence generated in the –RT reactions from the sample reactions which amplified transcript from RNA template.

Relative transcript levels of each target were significantly and consistently higher in fasted compared to fed mice groups (p < 0.0001, Figure 5.6.2) In particular, transcript for T1R2 was present in fasted mice at levels on average 33 times higher than in the fed mice. Mucosal levels of T1R3 transcript in fasted mice were increased 5-fold, $G\alpha_{gust}$ levels 35 fold and TRPM5 levels 14 fold compared to those in fed mice.

β-actin was used as the reference gene as experimental samples were from the same tissue type and were confirmed not to be significantly different in β-actin levels in preliminary experiments.
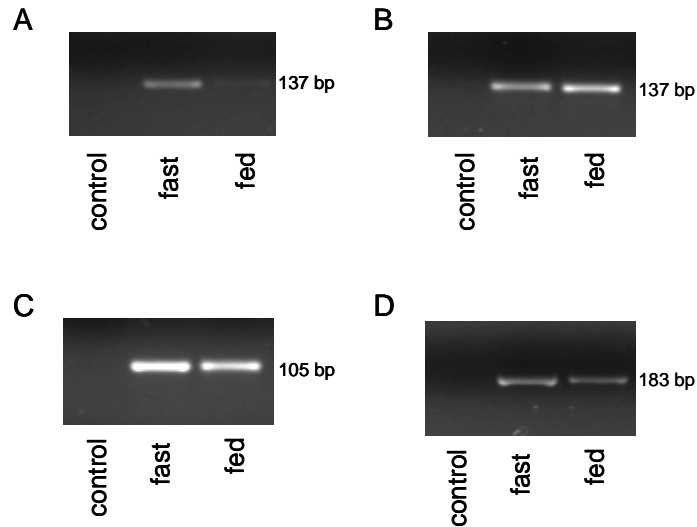
Figure 5.6.1 Gel electrophoresis showing specific taste PCR products amplified from fed and fasted mucosal RNA samples.
Real time RT-PCR reactions with specific primers for T1R2, T1R3, Gα_{gust} and TRPM5 were performed using RNA template obtained from jejunal mucosal samples from fed and fasted animals. Melt curve analyses indicated the existence of a single specific product. To further confirm specificity, PCR products from selected reactions were additionally run on ethidium bromide gels using electrophoresis and visualised under UV light. A single band corresponding to the predicted product size was observed for T1R2 (A), T1R3 (B), Gα_{gust} (C) and TRPM5 (D) and no bands were visible in control reactions where RNA template was substituted with nuclease-free water. For some products, particularly those amplified with T1R2 primers, the higher transcript levels found in fasted tissue samples is reflected in a greater intensity of the gel band.
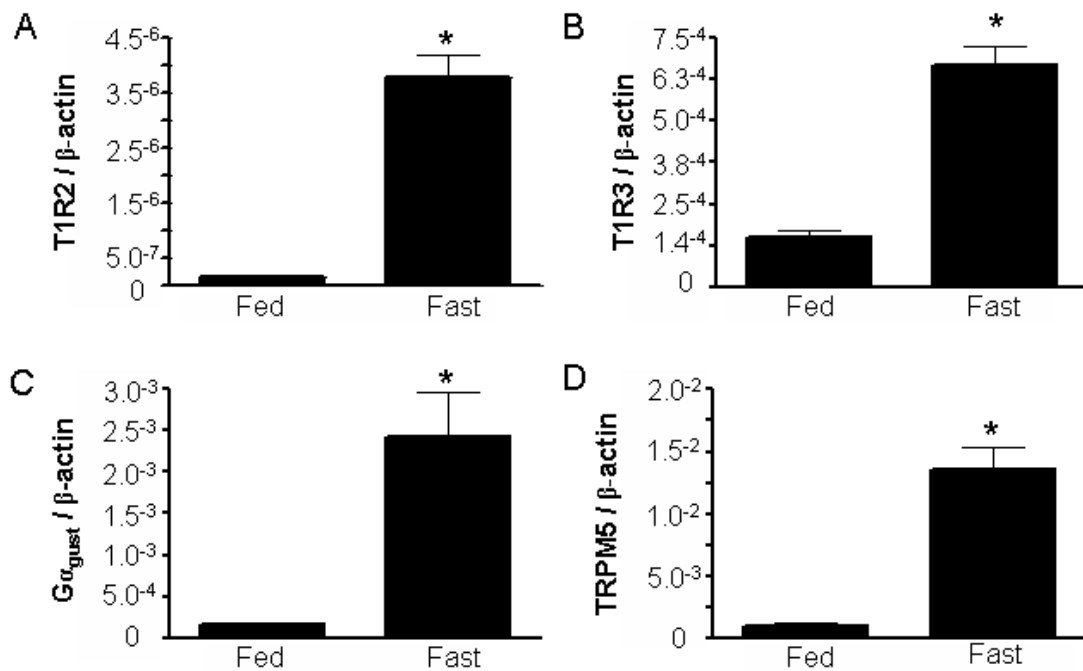
Figure 5.6.2 Taste transcript levels in jejunal mucosa from fed and fasted mice.
Real time RT-PCR expression data of each taste transcript level relative to β-actin levels are compared in jejunal mucosa RNA samples from 16 hour fed or fasted mice (n = 6 per group). In the case of all taste transcripts, expression levels were significantly higher in mucosal samples from fasted compared to fed animals (n = 6 per group, p<0.0001). Transcript levels in the fasted mucosal samples for T1R2 were on average 33-fold higher than fed samples (A), T1R3 levels were 4.5-fold higher (B), $G\alpha_{gust}$ was an average 35 times higher in fasting (C) and TRPM5 transcript levels were14-fold higher in fasted compared to fed mucosa (D).

5.6.2 Relative expression of Tph-1 and Gcg in jejunal mucosa from fed and fasted mice

Tph-1 and Gcg transcripts were specifically expressed in the jejunal mucosa in fed and fasted mice. Melt curve analyses indicated the existence of a single product in reactions using mucosal RNA template and the absence of primer dimers (Figure 5.6.3). The specificity of PCR products was further confirmed by gel electrophoresis showing that only a single band of the predicted amplicon size of each target was present in the reaction (Figure 5.6.4). Tph-1 was expressed at low levels in the mouse jejunal mucosa, and was frequently below the threshold of detection for real time RT-PCR and represented the least abundant transcript in these experiments. In contrast, transcripts for glucagon were present in moderate levels.

Quantitative expression data indicated that Tph-1 transcript levels were 10 fold higher in mucosal samples from fasted compared to fed mice ($p < 0.0001$, Figure 5.6.5). In contrast, there was no significant difference in transcript levels of Gcg between fed and fasted mice.
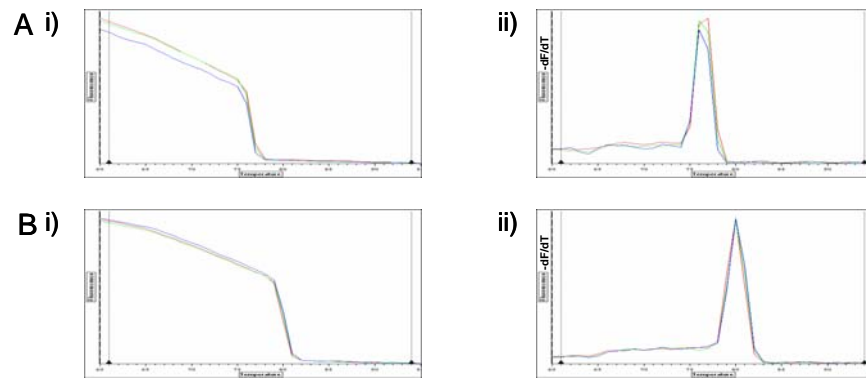
Figure 5.6.3 Melting curve analyses for Tph-1 and glucagon product characterisation.
In all samples at completion of the real time cycler programme a melting curve for each reaction was obtained. The melting curves for samples amplifying Tph-1 (A) and glucagon (B) are shown (i), these curves show the characteristic temperature-dependent decrease in fluorescence levels as double stranded products denature followed by a steep decline as the melting temperature (T_m) is reached. The negative derivative (-dF/dT) of the melting curve (ii) shows a single peak indicating a single T_m and therefore amplification of a single product. This validated that no non-specific products were co-amplified in Tph-1 and glucagon reactions and confirmed the absence of primer dimers.
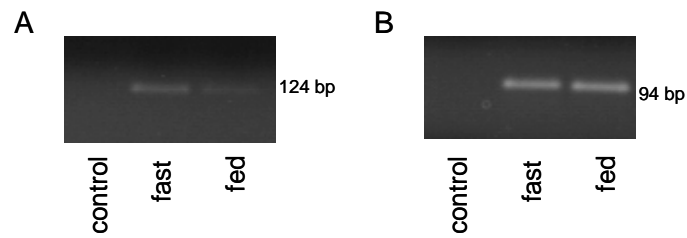
A   124 bp

control   fast   fed

B   94 bp

control   fast   fed

Figure 5.6.4 Gel electrophoresis assessment of Tph-1 and glucagon PCR products amplified from fed and fasted mucosal RNA samples.

Real time RT-PCR reactions using RNA template extracted from fed and fasted jejunal mucosa with primers specific for mouse Tph-1 and glucagon genes. PCR products were separated by electrophoresis on an ethidium bromide gel confirming a single band of the predicted product size for both Tph-1 (A) and glucagon (B) amplicons. Control reactions where RNA template was omitted and substituted with nuclease-free water did not result in amplification of any product. Real time expression data showed Tph-1 to be expressed at significantly higher levels in the mucosa of fasted mice compared to the fed. This is additionally indicated in the gel where the band corresponding to the Tph-1 amplicon from a fasted sample appears to be more intense, suggesting the presence of more product, than in the fed sample.
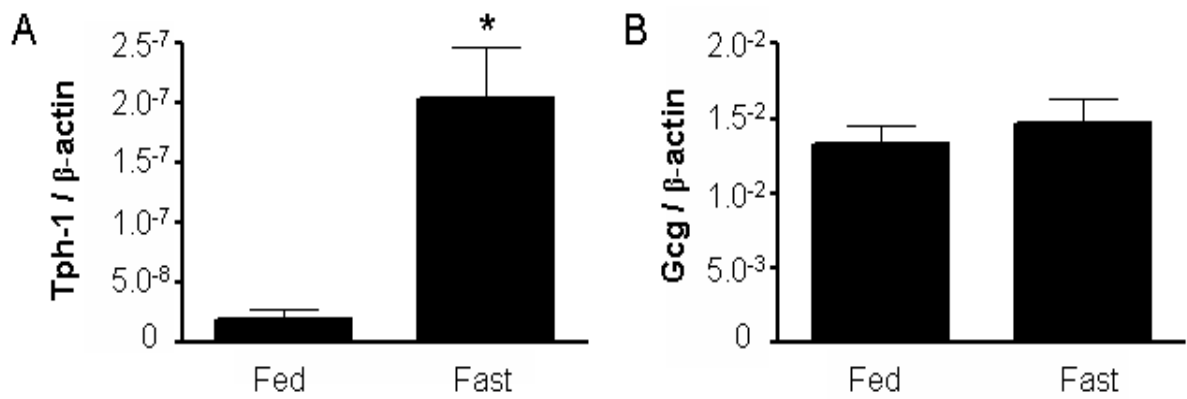
Figure 5.6.5 Tph-1 and glucagon transcript levels in jejunal mucosa from fed and fasted mice.
Real time RT-PCR expression data of Tph-1 (A) and glucagon (B) transcript levels relative to β-actin in jejunal mucosa RNA samples from 16 hour fed or fasted mice. Tph-1 overall was expressed only at very low levels in the jejunum. However Tph-1 was found to be expressed at significantly higher levels in fasted samples compared to fed (p < 0.001), with fed levels, on average, 10-fold lower than in fasting. Glucagon transcript levels were not significantly different between fed and fasted samples. N = 6 per group, Mean ± SEM.

5.6.3 Relative expression of 5-HT$_3$R and GLP-1R in nodose ganglia from fed and fasted mice

Transcripts for both 5-HT$_3$R and GLP-1R were identified in the nodose ganglion of fed and fasted mice. Melt curve analyses confirmed the existence of a single specific product (Figure 5.6.6) with no primer dimers indicating that all fluorescence produced and measured in real time reactions was due to SYBR green binding to the specific amplicons of interest. No product was amplified in control reactions.

Quantitative analysis of 5-HT$_3$ receptor transcript expression in mouse nodose ganglia showed that transcript levels were 3 fold lower in fasted compared to fed mice ($p < 0.001$). Transcript levels of the GLP-1 receptor also differed between experimental samples, and were nearly 2 fold higher in nodose ganglia from fasted, compared to fed mice ($p < 0.01$, Figure 5.6.7).
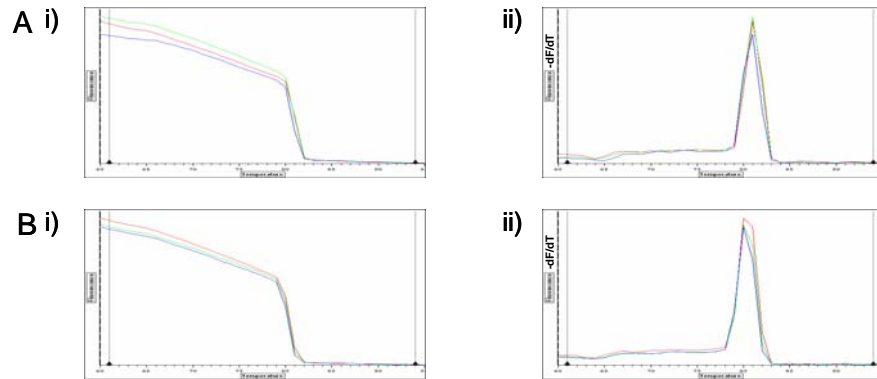
Figure 5.6.6 Melting curve analyses for 5-HT$_3$R and GLP-1R product characterisation.
In all samples at completion of the real time cycler programme a melting curve for each reaction was obtained. The melting curves for samples amplifying 5-HT$_3$R (A) and GLP-1R (B) are shown (i). The curves show the characteristic temperature-dependent quench in fluorescence levels and steep decline as the melting temperature (T$_m$) is reached. The negative derivative (-dF/dT) of the melting curve (ii) shows a single peak indicating a single T$_m$ and therefore amplification of a single product. This confirmed that no non-specific products were co-amplified in Tph-1 and glucagon reactions and there were no primer dimers formed, thus validating the specificity of the assay.
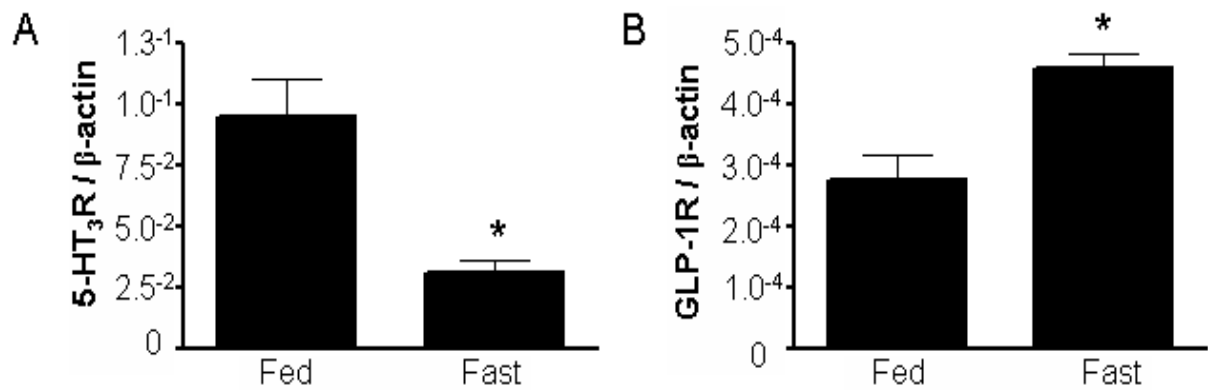
Figure 5.6.7 5-HT$_3$R and GLP-1R transcript levels in nodose ganglia from fed and fasted mice. Real time RT-PCR expression data of 5-HT$_3$R (A) and GLP-1R (B) transcript levels relative to β-actin in nodose ganglion RNA samples from 16 hour fed or fasted mice. 5-HT$_3$R transcript expression was an average of 3 times higher in fed nodose RNA samples compared to fasted ($p < 0.001$). Conversely GLP-1R expression was approximately 1.5 times higher in ganglia from fed mice compared to fasted ($p < 0.01$). Mean ± SEM, N = 6 per group.

5.7 Discussion

The regulatory mechanisms that govern gastric emptying rate in response to intestinal nutrient have been shown to rapidly adjust to specific and previous dietary intake. Such adaptation could result from alterations in the number or sensitivity of molecules involved in nutrient feedback pathways from the gut lumen. This adaptation may occur at several levels, in the receptive mechanisms of the primary sensor cells, through release of local mediators or at mediator detection by receptors on vagal afferents. This study focussed on key taste and signal molecules that may be involved in these stages of intestinal nutrient feedback and compared their expression in tissues from fed and fasted mice.

The potential detectors of intestinal sugars, the sweet taste receptors T1R2, T1R3 and their signal transduction counterparts $G\alpha_{gust}$ and TRPM5, were expressed at higher levels in the mucosa from fasted compared to fed mice. These results indicate that mucosal expression of taste molecules are up-regulated by fasting, or conversely, down-regulated during feeding. Functional studies show that a short-term diet high in glucose accelerates gastric emptying in response to subsequent intestinal glucose (63, 143), providing a compensatory mechanism to maintain glucose homeostasis in response to dietary changes (143). Accelerated gastric emptying may result from reduced feedback from intestinal nutrient receptors due to a downregulation of receptor numbers by prior high glucose exposure levels. The current study has established that expression of sweet taste receptor and signal transduction molecules are reduced in the intestinal mucosa after a short-term nutrient-rich diet, in comparison to fasting. As a consequence, if expression differences seen here are translated to changes in protein expression, these taste molecules may subserve changes such as gastric emptying rate with subsequent consumption. Particularly if T1R2/T1R3 receptive mechanisms do link into feedback pathways governing gastric emptying, a decrease in expression due to previous high nutrient intake would result in stimulation of less receptors (ie less feedback) by the next feeding. This would result in gastric emptying rate being comparatively accelerated,

meaning absorption of glucose would be less complete helping to maintain blood glucose levels and glucose homeostasis. Whereas increased T1R2/T1R3 receptor expression resulting from a fasted state would mean that when food is finally consumed it will result in exaggerated feedback leading to a slower rate of gastric emptying. This would allow the meal to have maximum transit time through the intestine and allow absorption of as much nutrient as possible to relieve the fasting state.

Studies investigating short-term effects of modified diet on gastrointestinal function have typically investigated gastrointestinal function following 4 or more days of dietary intervention. In this timeframe the villus epithelium has been renewed and regulatory changes, such as increased expression of glucose transporters in absorptive cells, have occurred. It is well described that the inhibition of gastric emptying by nutrients is dependent on the length of intestinal nutrient exposure (188). As a result, the increased rate of gastric emptying following a 4 day high-glucose diet may occur due to a reduced length of intestinal exposure of glucose, as glucose absorption is increased in the proximal small intestine in proportion to increased transporter capacity. This study, however, has shown that transcriptional changes in taste molecules in the intestinal epithelium occur over a shorter timeframe, inconsistent with complete epithelial renewal. This provides strong support to the hypothesis that intestinal taste receptors and signal molecules subserve the rapid adaptation in intestinal nutrient feedback to a changing luminal environment.

The assumption inherent in interpreting quantitative RT-PCR data is that detected changes are reflected by equivalent changes in protein abundance, and it has been shown that mRNA abundance is not always directly correlated with protein abundance (114). As a result, an investigation of relative protein abundance for these intestinal taste molecules in fed and fasted mice would be required to confirm these expression data. Indeed, alternate post-transcriptional processing mechanisms may participate in nutrient adaptation, however a direct effect of dietary status on intestinal taste molecule expression has been established in these studies.

The enteroendocrine cell products, 5-HT and GLP-1, are local mediators which may be released from the intestinal mucosa in response to intestinal carbohydrate and may subserve vagally mediated slowing of gastric emptying (155, 269). Quantification of transcript levels of the biosynthesis marker of 5-HT (Tph1) and precursor marker of GLP-1 (Gcg) in fed and fasted mice was undertaken to gauge any alterations in mediator production in response to dietary changes. A number of investigators have shown that expression of gut peptides can be altered by previous nutrient exposure patterns (55, 56, 151). Tph-1 transcript levels in the current study were present at low abundance in the intestinal mucosa but were significantly higher in fasted compared to fed mice, similar to expression changes seen with taste molecules. The 5-HT content of the stomach and intestine of mice has previously been shown to increase following a 24 or 48 hour fast (30). This directly supports current findings and suggests that increased fasting expression of 5-HT may be due to an increase in mucosal biosynthesis by Tph1 enzymes. Moreover, it provides evidence that variations in intestinal 5-HT in response to altered diet may be one mechanism by which gastric emptying responses adapt to dietary factors, however that 5-HT is a key signalling molecule in many gastrointestinal processes should be kept in mind.

Transcript levels of Gcg in the intestinal mucosa did not differ between fed and fasted mice in the current study. It is well established that the glucagon gene encodes the proglucagon derived peptides glucagon, GLP-1, GLP-2, glicentin and oxyntomodulin, which are produced by alternative post-translational processing in L-cells (74, 182). As a consequence, Gcg transcript levels may not accurately reflect levels of mucosal GLP-1, and a quantitative assay for GLP-1 protein would to required to investigate changes in mucosal expression. A previous study by Hoyt and colleagues has shown that proglucagon mRNA levels decreased by up to 40% in the jejunal mucosa in rats following a 3 day fast (151) and normalised with refeeding. This decrease in proglucagon mRNA directly correlated with decreases in plasma levels of GLP-1 (151). The

lack of difference in the current study suggests that transcriptional changes in Gcg may occur in response to longer periods of fasting. Indeed a comparative study in heifers faster for 48 hours showed reduced blood levels of GLP-1 but no changes in proglucagon mRNA abundance (334) This regulation of GLP-1 production in response to dietary status is therefore opposite to that of 5-HT and may highlight important differences in the roles of these signalling molecules and their regulation in response to nutritional status.

GLP-1 secreting L-cells are predominantly located in the distal small intestine and colon (84) however GLP-1 functions as an incretin and enterogastrone suggesting a role more suited to release from the proximal small intestine. Although there is evidence that neurohormonal mechanisms may link the proximal gut to distal GLP-1 release (5, 80, 284), L-cells are present throughout the small intestine (345) and increased expression of proglugagon in the proximal gut may occur specifically in times of feeding to facilitate the postprandial actions of GLP-1. Indeed, Hoyt and colleagues found that the magnitude of change in proglucagon mRNA levels in response to a 3 day fast was not nearly as pronounced in the ileum as the jejunum (151) indicating that GLP-1 may be subject to greater regulation in the upper gut.

Finally, changes in nutrient feedback pathways may also occur at the level of the specific receptors expressed on the vagal afferent terminals exposed to local mediator release. It is well described that vagal afferents show extensive expression of receptors for gut peptides that are either satiating or orexigenic in nature. Recently it has been shown that at least some of these receptors are regulated adaptively by alterations in nutritional state, and interact with one another to promote or reduce food intake (34-36). For example expression of receptors for cannabinoids, a known appetite stimulant, increase in the nodose ganglion of fasted rats (34) and this change is blocked by administration of cholecystokinin (CCK), a satiating peptide released in response to meal digestion which acts via the vagus nerve.

The expression of 5-HT$_3$R in the nodose of fed and fasted mice was investigated in the current study due to its putative role in mediating carbohydrate-induced regulation of gastric emptying (269). Nodose expression of 5-HT$_3$R was significantly lower in fasted mice compared to fed mice, in direct contrast to the mucosal expression of the 5-HT biosynthesis marker Tph1. There is experimental evidence that 5-HT$_3$R participate in triggering vagally mediated satiation in response to intestinal glucose in rodents (301), an effect that is synergistically enhanced by CCK signals (302). As such, a reduction in 5-HT$_3$R expression in fasted mice may relate to its role as a satiating factor, to prevent overt nutrient feedback when sustained consumption of food is favourable, such as after an extended fast. 5-HT levels in the gut however appear to be increased in fasting and there may be a balancing act between expression of signal molecules and receptors.

GLP-1 is a potent satiety factor released after meal ingestion (125) and the GLP-1R has recently been shown to be expressed in the nodose ganglion of rats (234). The current study has extended these findings in rodents using real time RT-PCR and has established that GLP-1R are also expressed in the nodose ganglion in mice. GLP-1R transcript levels also differed significantly between fed and fasted mice, with higher GLP-1R expression in fasted mice. Nodose and mucosal RNA samples in this study were obtained at a single timepoint following a 16 hour feed or fast - it would be interesting to observe changes in GLP-1R levels at varied time points to provide a more dynamic picture of receptor regulation. Plasma levels of GLP-1 and 5-HT after a meal or glucose ingestion appear to follow different timecourses. 5-HT levels do not rise above basal levels until around 60 minutes following a meal (150), with peak levels reached hours after meal ingestion, suggesting a slow, sustained presence of 5-HT circulating for hours after feeding. On the other hand in response to oral ingestion of glucose plasma levels of GLP-1 peak rapidly within 30 minutes then decline to baseline (307). These more transient circulating levels of GLP-1 may produce a different pattern of regulation of receptor gene transcription than the more prolonged circulating 5-HT levels, such that GLP-1 exposure to vagal afferents is not sufficient to induce GLP-1R down regulation in contrast to the

prolonged effect of 5-HT. It should also be considered that any changes in receptor mRNA expression in the nodose, if this leads to up-regulation of receptor protein, will incur an extra time delay in the transport of these newly synthesised receptors down to the afferent terminals. This time delay may or may not allow these changes to occur in synchronisation with nutritional status but further study of protein levels over time would be required to establish this. However it appears that the intestinal epithelium itself is able to respond to short-term nutritional status and these changes may be rapidly implemented at the luminal surface.

In summary, this study provides direct evidence that the expression of taste and signalling molecules likely to be involved in intestinal nutrient detection can be rapidly altered according to nutritional status. Further studies will be needed to determine which specific dietary components exert the most potent effects on the expression of mucosal taste receptors, however the results of this study suggest that adaptations in gastrointestinal functions in response to increased nutrient loads may be linked to changes in expression of sweet taste molecules in the intestinal mucosa as well as changes in the signalling mechanisms to vagal afferents.

6. EXPRESSION OF TASTE MOLECULES IN THE UPPER GASTROINTESTINAL TRACT IN HUMANS WITH AND WITHOUT TYPE 2 DIABETES

6.1 Summary

Background: The molecular mechanisms that faciltate the detection of carbohydrate in the human small intestine have not been identified, however, alterations in these receptive mechanisms may underlie the frequent disturbances in postprandial gastric motility associated with diabetes mellitus. Sweet taste receptors and transduction molecules are expressed in the rodent intestine and may be involved in regulating gut function but their presence in the human upper gastrointestinal tract has not been explored. *Aims:* To localise and quantify expression of taste molecules in regions of the human upper gastrointestinal tract, and determine whether their expression is altered in type 2 diabetes. *Methods:* Endoscopic mucosal biopsies from multiple regions of the upper gastrointestinal tract were obtained with consent from patients with and without diabetes undergoing surveillance endoscopy after an overnight fast. Real time RT-PCR was used to determine absolute expression levels of T1R2, T1R3, Gα_{gust} and TRPM5 in individual biopsies. Immunohistochemistry was used to localise Gα_{gust}. *Results:* Taste molecules were expressed in the human gastrointestinal mucosa and preferentially expressed in the proximal small intestine compared to the stomach ($p > 0.01$). Immunolabelling for Gα_{gust} in duodenal biopsies confirmed labelling in solitary cells dispersed throughout the epithelium. Expression of taste molecules in duodenal biopsies did not differ between patients with and without diabetes however expression of T1R2 ($P < 0.05$), T1R3 ($P < 0.05$) and TRPM5 ($p < 0.01$) correlated inversely with the blood glucose concentration in patients with type 2 diabetes. *Conclusions:* Taste molecules are expressed with regional specialisation in the human upper gastrointestinal mucosa, consistent with a role in nutrient 'tasting'. In type 2 diabetes, lower expression

levels coincide with elevated blood glucose concentration, suggesting that intestinal 'taste' signalling is under dynamic metabolic control.

6.2 Introduction

The molecular identity of the nutrient receptive mechanisms which initiate feedback signals to facilitate digestive processes in the human small intestine has not been revealed. The studies in this thesis have established that taste molecules tuned to detect sugars in taste receptor cells of the tongue are also expressed throughout the gastrointestinal tract in mice. The heterodimeric G-protein coupled receptors T1R2 and T1R3, chemosensory G-protein $G\alpha_{gust}$ and taste transduction ion channel TRPM5 are all expressed in the mouse intestinal mucosa. Furthermore immunolabelling with a primary antibody for $G\alpha_{gust}$ suggests the presence of epithelial 'taste' cells. A portion of $G\alpha_{gust}$ immunopositive cells in the mouse jejunum co-express 5-hydroxytryptamine (5-HT) and glucagon-like peptide 1 (GLP-1), gut hormones involved in intestinal carbohydrate-induced delayed gastric emptying. It is unknown, however, whether taste molecules are expressed in equivalent manner in the upper gastrointestinal tract of humans and whether they are co-expressed in enterochromaffin or L cells and if so whether to a greater or lesser extent than mice.

Understanding of nutrient sensing mechanisms in the human gut may be key to understanding or intervening in abnormal gastrointestinal function associated with diabetes mellitus. Both upper gastrointestinal symptoms (39, 313) and disordered motility (144, 149) are common, with delayed gastric emptying observed in 30-50% of Type 1 and 2 patients (149). Current knowledge of the underlying pathophysiology of delayed gastric emptying in diabetes is limited but can not be directly attributed to myopathy or neuropathy (149, 373) and is exacerbated by hyperglycemia (312). A potential underlying

cause of postprandial delayed gastric emptying may be abnormal feedback from the small intestine (187) leading to excessive signals which prolong gastric emptying time and cause symptoms such as early satiety. Although not well studied in diabetes (277), heightened perception of intestinal nutrients contributes to alterations in sensory and motor functions in functional dyspepsia (12, 316). Alterations in the expression of mucosal chemosensory molecules may contribute to such inappropriate feedback in diabetes mellitus.

In the human gastrointestinal tract, $G\alpha_{gust}$ and members of the G-protein coupled T2R receptor family responsible for the detection of bitter compounds have been shown to be expressed in the colonic mucosa (294). In addition, immunoreactivity for $G\alpha_{gust}$ has also been identified in single colonic epithelial cells which coexpress GLP-1 or peptide YY in humans. However the expression of taste receptors which specifically detect sugars have not been investigated in the human upper gastrointestinal tract. Detailed information on the regional expression of taste molecules in the human upper gastrointestinal tract will indicate the relative importance of taste mechanisms at sites relevant to the triggering of nutrient feedback reflexes. This study in the human gastrointestinal tract was under taken in a manner similar to that used to investigate sweet taste molecule expression in the mouse gastrointestinal mucosa. However human biopsy tissue is reported to show a high level of sample to sample variation in expression levels of commonly used real time RT-PCR reference genes including 18S rRNA (349). Therefore a method for the absolute quantification of transcript levels within the RNA mass of the sample was adapted for use with human biopsy samples.

Expression information on taste molecules in the human small intestine will permit investigation of whether altered expression is associated with diseases that display gastrointestinal sensory and motor dysfunction, such as diabetes

6.3 Aims

1. To characterise the expression and location of taste molecules in the human upper gastrointestinal tract.

2. To evaluate expression of taste molecules in patients with type 2 diabetes.

6.4 Specific hypotheses

1. Taste molecules T1R2, T1R3, $G\alpha_{gust}$ and TRPM5 are expressed in the human upper gastrointestinal tract with regional specification relevant to nutrient feedback.

2. Expression of some or all sweet taste molecules in the duodenum are altered in patients with type 2 diabetes compared to non-diabetic patients.

6.5 Materials and methods

The study was approved by the Human Research Ethics Committee of the Royal Adelaide Hospital, Adelaide, Australia, and each subject gave written, informed consent.

6.5.1 Collection of human upper gastrointestinal biopsies

Human gastrointestinal mucosal biopsies for use in molecular studies were collected into RNA stabilisation reagent RNA*later* (Qiagen, Sydney, Austrailia) and kept overnight at 4ºC before storage at -20ºC until RNA extraction.

Enteroscopy biopsies in non-diabetic patients

Six non-diabetic subjects (mean age 63.6 years ± standard error 13.7, body mass index (BMI) 30.5 ± 2.4 kg/m^2) were recruited amongst patients referred to the Endoscopy Unit of the Royal Adelaide Hospital for push enteroscopy, in most cases for the investigation of bleeding of obscure origin. Five of the six patients had documented comorbidities that included ischemic heart disease (4 patients) and rheumatoid arthritis (1 patient). In all patients the small intestinal mucosa was macroscopically and histologically normal. Push enteroscopy was performed under conscious sedation with intravenous midazolam and fentanyl, after at least 8 hours fasting. The enteroscope was passed as far distally in the jejunum as possible (mean straightened depth 167 ± 25 cm from the incisors) and two mucosal biopsies were taken at this level using standard biopsy forceps (designated 'mid-jejunum' or 'm'). The enteroscope was then withdrawn, and two further biopsies were taken at approximately the ligament of Treitz (proximal jejunum, 'p'), and in identical manner, from the second part of the duodenum, gastric antrum, body and fundus, and the distal esophagus.

Endoscopy biopsies in patients with type 2 diabetes

Seven subjects with type 2 diabetes (mean age 67.9 ± 2.9 years, BMI 32.7 ± 2.1 kg/m^2) were recruited amongst patients referred for diagnostic endoscopy, in most cases to investigate iron deficiency. The mean duration of diabetes was 16.3 ± 3.6 years, and all were taking metformin, with or without additional oral hypoglycaemic agents or insulin. Five had microvascular complications (peripheral neuropathy in all five, nephropathy without elevated creatinine in three, and retinopathy in one), and all but one had evidence of macrovascular disease. As a group, they had few upper gastrointestinal symptoms, based on a standard questionnaire that rated anorexia, nausea, early satiation, upper abdominal discomfort, vomiting and pain each on a scale of 0 (none) to 3 (severe), with scores added to derive a total symptom score (mean

3.6 ± 1.4 from a maximum possible score of 18). Their glycated hemoglobin (HbA1c) was 7.9 ± 0.3 %, and the blood glucose concentration measured by glucometer (Medisense Precision QID; Abbott Laboratories, Bedford, MA) immediately prior to endoscopy was 7.3 ± 0.7 mmol/L. At endoscopy, two mucosal biopsies were taken from the second part of the duodenum.

6.5.2 Absolute quantification of taste molecules

<u>RNA extraction</u>

Gastrointestinal mucosal biopsies were removed from RNA*later* before being snap frozen in liquid nitrogen. Individual biopsies were transferred to a glass mortar and pestle to mechanically disrupt the tissue. Homogenisation of tissue was achieved using a QIAshredder column (Qiagen) and RNA extracted using the RNeasy Mini kit (Qiagen) in an identical protocol used for RNA extraction from mouse tissues described in detail in Chapter Two. The on-column DNase digestion treatment was included to remove contaminating genomic DNA. Purified RNA was quantified in triplicate by spectrophotometer (260 nm) and purity assessed by the A_{260}/A_{280} ratio. Aliquots of RNA template were stored at -80°C until use.

<u>Primers</u>

Primers for the specific detection of human taste molecule genes T1R2, $G\alpha_{gust}$ and TRPM5 as well as endogenous controls β-actin and 18S rRNA were purchased commercially as validated QuantiTect primer assays (Qiagen). Schematic representations of the amplified regions of each gene detected with the specific primer assays are shown in Figure 6.5.1. QuantiTect primer assay for T1R3 is reported to potentially coamplify contaminating genomic DNA therefore primers for T1R3 were designed using Primer

3.0 software (Applied Biosystems, Foster City, CA) based on the human gene sequence obtained from the NCBI nucleotide database. One primer of the pair was designed to span an exon-exon boundary as determined from exon information in the Ensembl gene database (www.ensembl.org). Specific information on all primers used for real time RT-PCR can be found in Table 6.5.1.

Table 6.5.1 Primers for amplification of human taste molecule genes in real time RT-PCR

Gene	Entrez gene ID	Accession no.	Length of transcript (bp)	Primer information	Amplicon length (bp)
T1R2 (TASR2)	80834	NM_152232	2521	QT01026508	94
T1R3 (TASR3)		NM_152228		Forward (5' to3'): caaaacccagacgacatcg	101
				Reverse (5' to 3'): catgccaggaaccgagac	
Gα$_{gust}$ (GNAT3)	346562	XM_294370	1065	QT00049784	111
TRPM5	29850	NM_014555	3913	QT00034734	115
18S rRNA (RRN18S)		X03205	1869	QT00199367	149
β-actin (ACTB)		NM_001101		QT00095431	146

QT, QuantiiTect primer assay (QIAGEN)

Figure 6.5.1 Approximate locations of the amplicon regions on human taste genes amplified by QuantiTect Primer Assays.

Validiated primer sets were purchased commercially from Qiagen as QuantiTect primer assays for human taste-signal genes. The exact primer and amplicon sequences are not revealed by the manufacturer but schematic representations of the location of the detected amplicon on the target gene sequences are shown for T1R2 (A), $G\alpha_{gust}$ (B), TRPM5 (C). Additional primers to detect these genes were specifically designed to flank either side of the region containing the QuantiTect primer assay amplicon by RT-PCR. These larger RT-PCR products containing the sequence detected by the commercial primer assays were purified and quantified for use as standards of known copy numbers to create the standard curve for absolute copy number determination of samples in real time RT-PCR. The sequence of the larger amplicons were known and as they specifically contained the QuantiTect primer amplicon further validate that these commercial primers detect the specific gene of interest.

Generation of RT-PCR products as standards for target gene absolute standard curves

Absolute standard curves were created as a template series in which the starting copy number in each reaction tube was known. To be used as a standard template nucleic acid must firstly contain the amplified target sequence and secondly the absolute quantity of the standard must be known. For this purpose RT-PCR products were generated and quantified. Additional primers for each taste molecule gene were designed to produce a larger amplicon which contained the specific region amplified by the primers used for real time RT-PCR. Details of these primers are given in Table 6.5.2.

Table 6.5.2 Primers to generate RT-PCR product containing target amplicons for use as standards

Gene	Forward primer (5'-3')	Reverse primer (5'-3')	Amplicon length (bp)
T1R2	tacctgcctggggattac	aaatagggagaggaagttgg	390
T1R3	agggctaaatcaccaccaga	ccaggtaccaggtgcacagt	953
$G\alpha_{gust}$	gaggaccaacgacaacttta	acaatggaggttgttgaaaa	491
TRPM5	cttgctgccctagtgaac	ctgcaggaagtccttgagta	639

RT-PCR was performed using RNA extracted from human duodenal biopsies with the one-step RT-PCR kit (Qiagen) according to the manufacturer's instructions as described in detail in Chapter Two (section 2.5.2.2). The subsequent RT-PCR products generated after 40 PCR cycles were separated by electrophoresis on an ethidium bromide 3% agarose gel. All reactions produced a specific band of the predicted product size for each target. These specific bands were then cut from the gel and the cDNA contained within it extracted using the Ultraclean™ DNA Purification Kit (MO BIO Laboratories, Inc., West Carlsbad, CA) following the manufacturer's protocol for extraction from agarose gels. Briefly the weight of the gel band slices in an eppendorf tube was determined and the appropriate volumes of ULTRA TBE MELT and ULTRA SALT from the kit was added and the tube then incubated at 55ºC until the gel was completely melted. 10µL of ULTRA BIND, DNA-binding silica solution, was added and left for 5 min with

intermittant mixing to allow maximal DNA to bind to the silica. The tube was centrifuged for 5 sec and the supernatant removed and discarded. The pellet was resuspended in 1 ml of ULTRA WASH solution by vortexing to remove any residual salt and melted agarose, again centrifuged and the supernatant again discarded. The pellet was resuspended in TE buffer and incubated at room temperature for 5 min to allow DNA to separate from the silica and into the elution buffer. After centrifugation for 1 min the supernatant was collected and the concentration of purified cDNA in solution was measured in triplicate by spectrophotometer.

Copy number calculations for cDNA standards

cDNA concentration was converted into copy numbers according to the formula for creation of standard curves from DNA templates provided online by Applied Biosystems (http://www.appliedbiosystems.com/support/tutorials/pdf/quant_pcr.pdf). Briefly, the mass (m) of a single cDNA molecule was determined by multiplying the fragment size (base pairs, bp) by a factor derived from the average molecular mass of a dsDNA molecule (660 g/mol) and Avogadro's constant (6.02×10^{23} bp/mol). Concentrations corresponding to a desired copy number were obtained by the following formula:

$$\text{concentration (g/µl)} = \frac{m \times (bp \times 1.096 \times 10^{-21}) \times \text{copy number}}{\text{reaction volume (µl)}}$$

Purified cDNA stock solution was diluted down to a workable concentration and then serial dilutions were created to contain 10^4, 10^5, 10^6, 10^7, 10^8 and 10^9 molecules in each dilution, in order to obtain a template for standard curve reactions.

Real time RT-PCR protocol

Real time RT-PCR was carried out using the QuantiTect SYBR Green one-step RT-PCR kit (Qiagen) in the same manner and under the same PCR cycling settings with a final melt curve analysis as in experiments using mouse tissue detailed in Chapter Two (section 2.5.2.7). The target assay for each RNA template was performed in quadruplicate. Additional reactions with primers for endogenous controls β-actin and 18S rRNA were included in each assay. A standard curve of triplicate reactions for each of six dilutions of the known standard template was inserted into the plate after the RT step for initial PCR activation. Control reactions were performed in which the RNA template was substituted with nuclease-free water and additional reactions were performed without the RT step to confirm lack of genomic DNA contamination. Specificity of PCR products were additionally confirmed by gel electrophoresis.

Data and statistical analysis

A standard curve based on the copy numbers of the known standards and threshold cycle (C_T) was automatically generated by the Opticon monitor (Biorad). The mRNA copy number for each target was calculated from C_T values, referenced to the standard curve. All four replicates were averaged for final mRNA copy number per patient, which was expressed as copies per total RNA sample mass. Statistical analysis of data was performed with Prism software (version 4.03; Graphpad, San Diego, CA). An unpaired t-test was used to compare expression between gastric and intestinal regions. Differences in duodenal expression of taste molecules in diabetic and non-diabetic patients were tested using a Mann Whitney test. Correlations between transcript expression and other factors were performed using a Spearman correlation giving a Spearman correlation coefficient (r). A P value < 0.05 was considered significant. Data were expressed as mean ± standard error.

6.5.3 Immunohistochemistry

Duodenal biopsies from two diabetic patients were collected in 10% neutral buffered formalin and fixed at room temperature (RT) for 1-2 hr. Biopsies were then washed in 0.1M phosphate-buffered saline (PBS) pH 7.4 before cryoprotection in 30% sucrose/PBS. Biopsies were embedded in cryomoulds and frozen before being sectioned at 10 μm on a cryostat (CRYOCUT 1800 Leica Biosystems, Nussloch, Germany) and thaw-mounted directly onto gelatin-coated slides. Immunoreactivity for $G\alpha_{gust}$ was detected with a C-terminus directed polyclonal rabbit antibody (1:200, SC-7782, Santa Cruz Biotechnology, CA, USA). Immunoreactivity for 5-HT was detected using a mouse monoclonal antibody (M0758, DakoCytomation, Glopstrup, Denmark, working dilution 1:100 and GLP-1 immunoreactivity was detected by a goat polyclonal antibody (SC7782, Santa Cruz Biotechnology, working dilution 1:100). Working dilutions were selected for best label with low background from a dilution series in preliminary assays.

Sections were air dried at room temperature for 15 min before several washes in PBST (PBS + 0.2% Triton X-100, Sigma-Aldrich, St Louis, MO) at pH 7.4. Sections were incubated with blocking solution (2% normal goat serum, 1% BSA, 0.1% Triton X-100, 0.05% Tween 20, 0.1% gelatine, 1 X PBS) for 1 hr at RT. Primary antibodies were diluted in blocking solution and incubated singly or in combination overnight at 4°C. Negative controls were obtained by omitting the primary antibody from the incubation. Sections were then washed in PBS-T and incubated with an anti-rabbit Alexa Fluor 546 secondary antibody (1:200 in PBS-T) singly or in combination with species specific Alexa Fluor 488 secondary antibodies for 1 hr at RT. Sections were washed again in PBS-T and mounted in ProLong Antifade reagent (Invitrogen) and coverslipped. Negative controls where primary antibody was omitted from the incubation were performed in every assay.

Sections were visualised and imaged on an epifluorescence microscope (BX-51, Olympus, Australia) and

images acquired on a monochrome CCD digital camera system (Photometrics CoolSNAP*fx*, Roper Scientific,Tuscon, AZ) using V++ Precision Digital imaging System software (Digital Optics, Auckland, New Zealand).

6.6 Results

6.6.1 Expression of taste molecules in the human upper gastrointestinal tract

Real time RT-PCR revealed that taste molecules T1R2, T1R3, $G\alpha_{gust}$ and TRPM5 were specifically expressed in the mucosa of the human upper gastrointestinal tract. Melt curve analyses of the reaction products confirmed that no primer dimers and one specific product were generated in reactions for each primer assay (Figure 6.6.1). Gel electrophoresis confirmed that PCR products in all assays corresponded to the predicted amplicon size and that the corresponding band was absent in control reactions that did not contain template or did not undergo reverse transcription (Figure 6.6.2). Absolute transcript copy number for each taste signal molecules were derived form the standard curves produced by the amplification of the known standards (Figure 6.6.3). Absolute transcript levels for T1R2, T1R3, $G\alpha_{gust}$ and TRPM5 in human duodenal biopsies are shown in Figure 6.6.4. $G\alpha_{gust}$ and TRPM5 transcripts were present in higher quantities than those of T1R2 and T1R3. $G\alpha_{gust}$ transcripts were 11.5 ± 3.6 fold higher than T1R3 in the human duodenal mucosa, while $G\alpha_{gust}$ was 27.7 ± 3.3 times more abundant than T1R2. T1R2 was the least abundant taste molecule transcript.
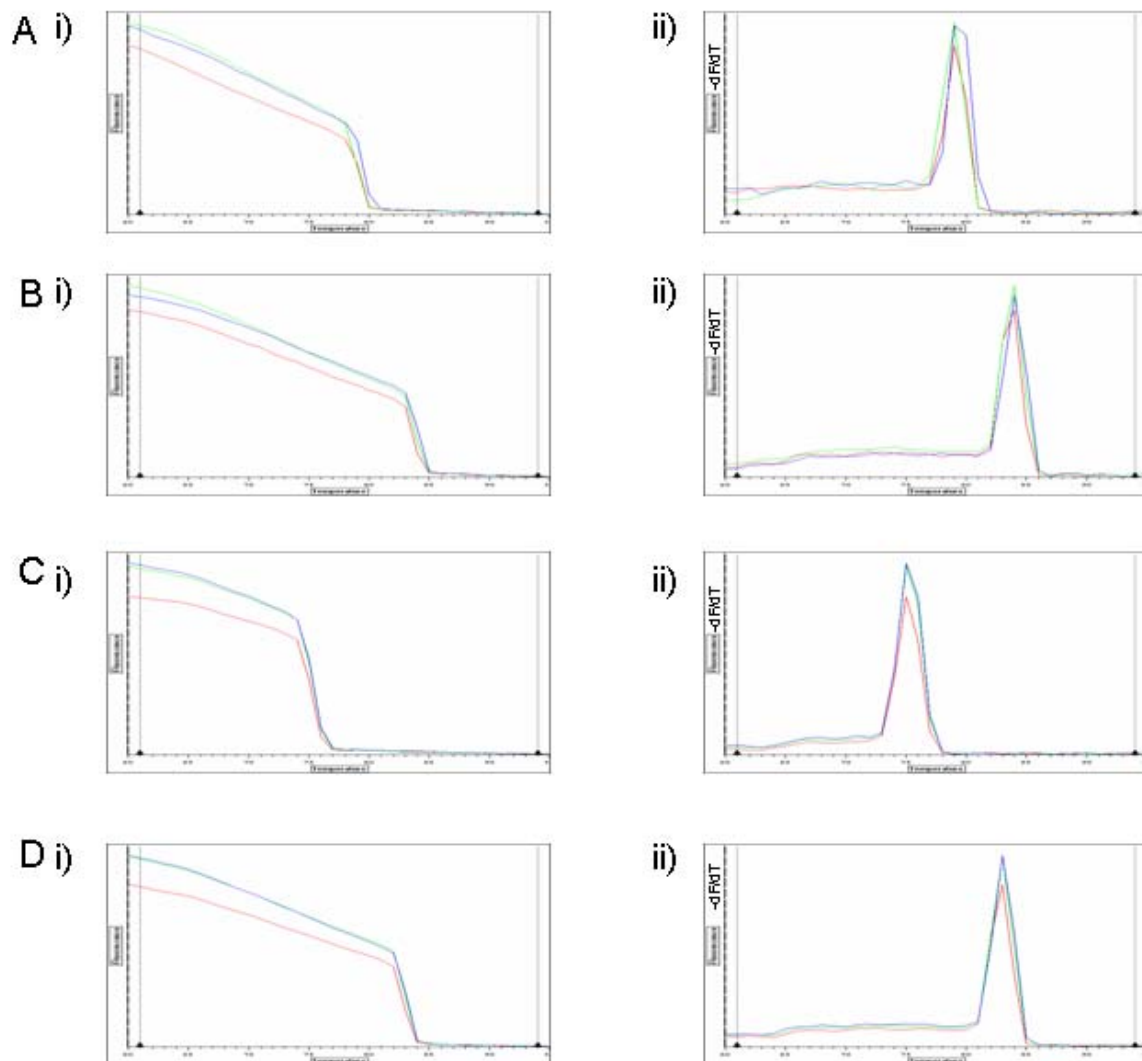
Figure 6.6.1 Melt curve analyses of generated human taste RT-PCR products.
RT-PCR showed that taste molecules are expressed in the human gastrointestinal mucosa. To confirm product specificity at completion of PCR cycling the programme was extended to measure fluorescence levels at temperatures from 60ºC to 90ºC to generate a melt curve for analyses. The melting curves for samples amplifying T1R2 (A), T1R3 (B), $G\alpha_{gust}$ (C) and TRPM5 (D) are shown (i). The fluorescence plots against temperature all show the characteristic decline in signal as the temperature increases and a sharp drop as the melting temperature of the product is reached. The plot of the first negative derivative (-dF/dT) of the melting curve for each product are shown (ii). The single peaks of the plots in each reaction confirm a single melting temperature and thus the amplification of a single specific product. These curves validate that no non-specific products were coamplified and additionally that no primer dimers were formed in the reaction.
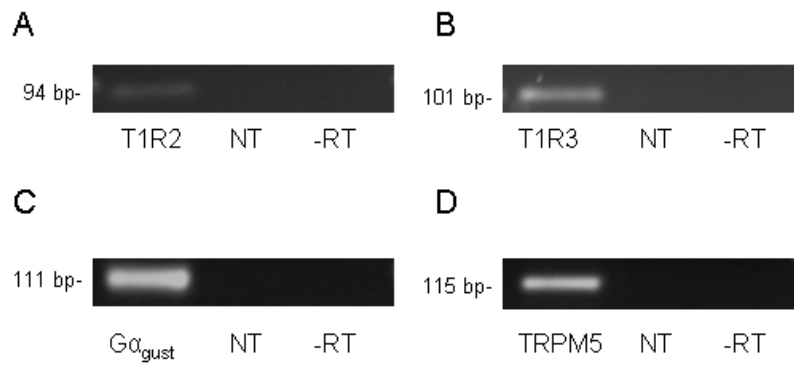
Figure 6.6.2 Specific expression of taste molecules in the human gastrointestinal tract shown by gel electrophoresis.
Gel electrophoresis of PCR products obtained using specific primer assays for taste molecules in real time RT-PCR with human gastrointestinal mucosal RNA template. A single band of the predicted product size can be seen in sample reactions for T1R2 (A), T1R3 (B), Gα_{gust} (C) and TRPM5 (D). No bands are seen in reactions where RNA template was substituted with nuclease-free water (NT) or when reverse transcription was omitted (-RT) confirming specific amplification from mucosal RNA template.
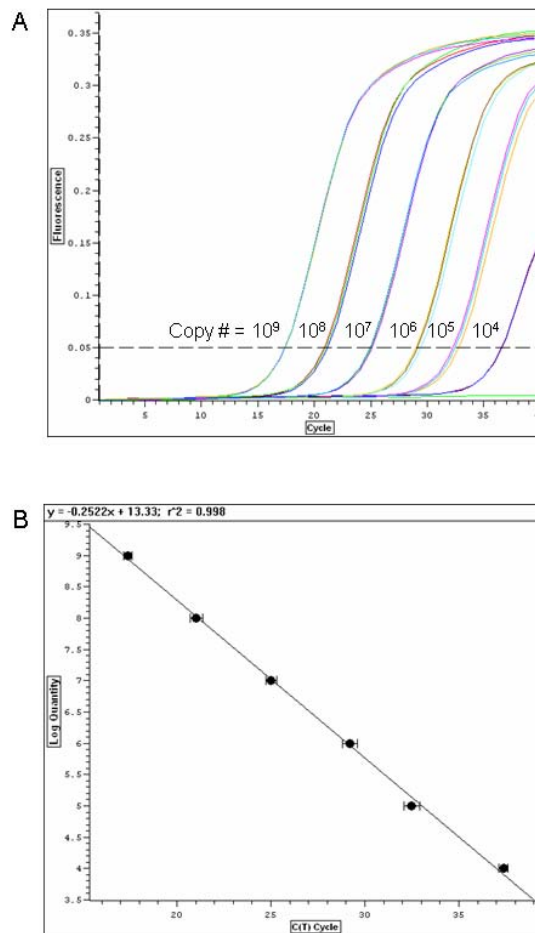
Figure 6.6.3 Example of a standard curve generated using standards of known copy number. Absolute quantification in real time RT-PCR requires that a series of reactions in which the starting template copy number is known is run in the plate with the samples to obtain a standard curve. PCR products containing the target sequence were used as standards. The concentration of the purified products was used to obtain a dilution series of six standards containing 10^4 to 10^9 copies in each tube. Real time PCR amplification curves are shown (A) for the triplicate reactions in each standard dilution. The standard containing the most copies (10^9) is first to reach threshold, successively followed by the next dilution until the lowest copy number standard crosses the threshold line. Often reactions containing 10^4 template copies did not reach the level of fluorescence needed to cross the threshold, indicating that samples containing less than 10,000 target transcripts would be below the threshold of detection for this technique. The cycle thresholds (C_T) of all targets in this study fell within the range of the standards. The mean C_T values of the standard replicates were converted to a standard curve graph (B) by the Opticon monitor software. The slope of the resulting linear plot is used to convert sample C_T values to copy numbers.
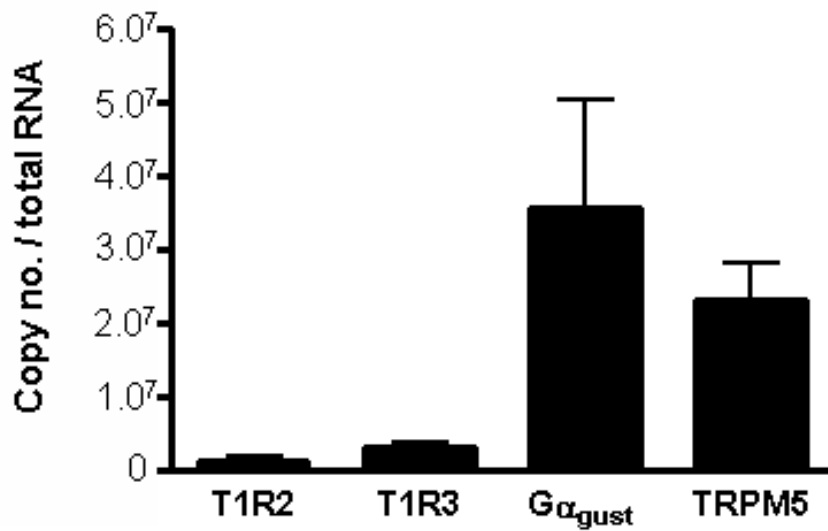
Figure 6.6.4 Expression levels of taste molecules in the human proximal intestine.
Absolute quantification by real time RT-PCR of taste transcripts in the human proximal small intestine are displayed to show the levels of each taste transcript. Individual taste molecules were present at different orders of magnitude. Comparison of absolute levels of taste molecule transcript in the duodenum showed that T1R2 and T1R3 were expressed at lower levels than $G\alpha_{gust}$ and TRPM5. Expression of $G\alpha_{gust}$ was 11.5 ± 3.6 fold higher than T1R3 and 27.7 ± 3.3 times higher than T1R2. T1R2 was the least abundant of all taste transcripts. N = 6, Mean ± SEM.

6.6.2 Regional specificity in expression of taste molecules in the upper gastrointestinal tract

Quantification of absolute copy numbers of taste molecule transcripts in upper gastrointestinal biopsies from the esophageal, gastric and intestinal mucosa of non-diabetic patients revealed distinct regional specificity in expression levels. The sweet taste receptor, T1R2, was present in the duodenum and jejunum, with a trend for decreased expression with increasing distance from the pylorus. No expression of T1R2 was detected in the distal esophagus or stomach (Figure 6.6.5A). The T1R common to the sweet and umami receptor, T1R3, was expressed in all regions of the upper gastrointestinal tract, but predominantly in the distal esophagus, duodenum and jejunum (Figure 6.6.5B). When assessed as gastric and intestinal samples T1R3 transcript levels were significantly higher in the proximal intestine (3.6 ± 0.8 fold, $p < 0.01$) than in the stomach (Figure 6.6.6B).

Transcript levels for $G\alpha_{gust}$ and TRPM5 showed similar expression profiles, with low levels detected in distal esophagus and stomach and prominent expression evident in proximal small intestine (Figure 6.6.5C, D). $G\alpha_{gust}$ mRNA levels were 70.3 ± 1.8 fold higher in proximal intestine than in stomach (N =7, $p < 0.001$, Figure 6.6.6C) while TRPM5 transcripts were 13.06 ± 1.6 fold higher in the proximal intestine (N = 7, $p < 0.001$, Figure 6.6.6D).
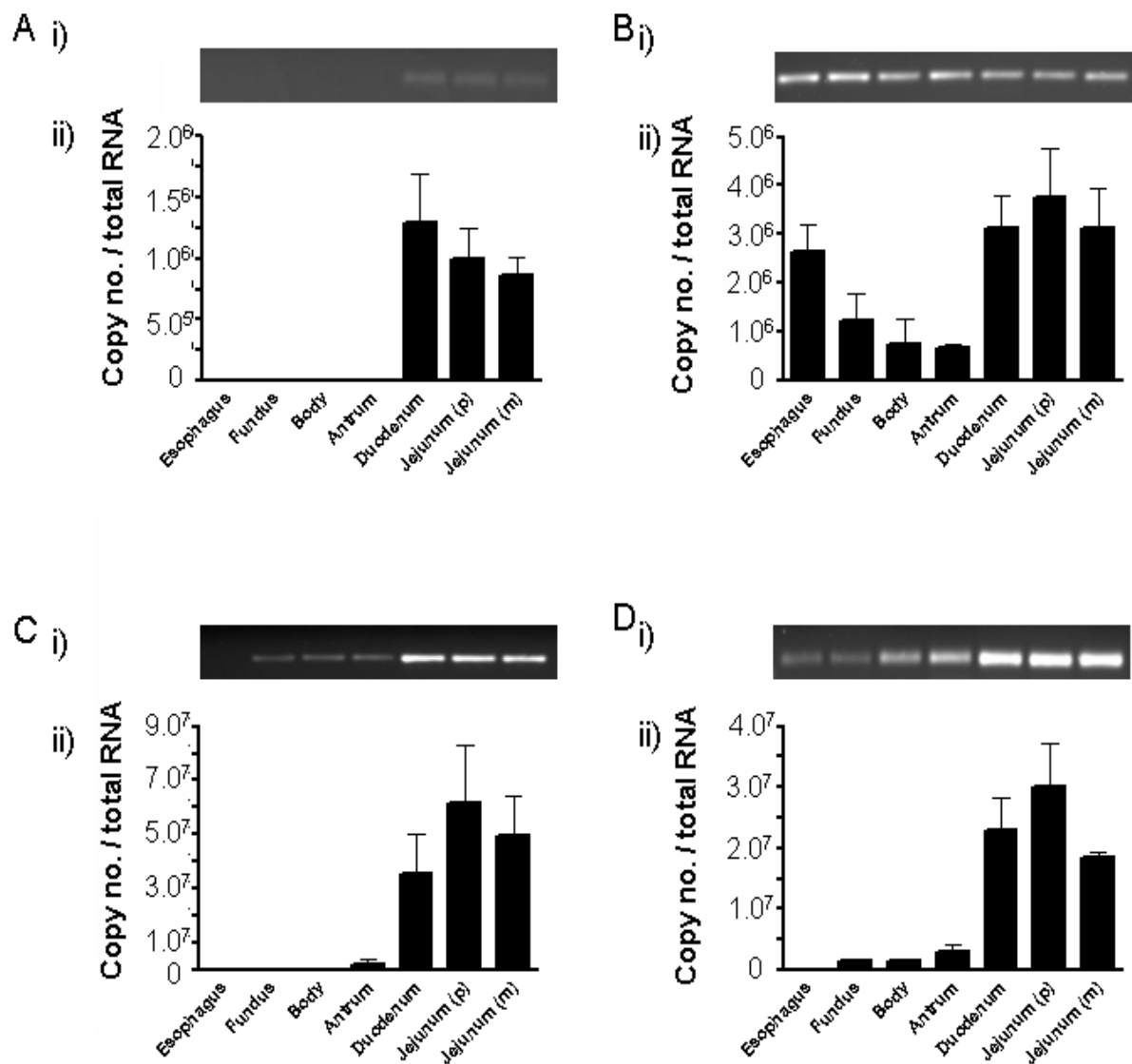
Figure 6.6.5 Regional expression of taste molecules in the human upper gastrointestinal tract. Absolute transcript levels of taste molecules T1R2 (A), T1R3 (B), Gα$_{gust}$ (C) and TRPM5 (D) were quantified by real time RT-PCR in mucosal biopsies from the distal esophagus, gastric fundus, body and antrum, duodenum, proximal jejunum (p) and mid jejunum (m) of non-diabetic 'control' patients. T1R2 transcripts were only present in intestinal biopsies and were not expressed in the esophagus or gastric regions as shown by gel electrophoresis of PCR products (Ai) and absolute transcript levels (Aii). T1R3 transcripts were detected in biopsies from all regions of the gastrointestinal tract (Bii) confirmed by gel electophoresis (Bi) which showed a band corresponding to the predicted amplicon size amplified from all samples. Regional expression levels of Gα$_{gust}$ (Cii) and TRPM5 (Dii) are shown. Gastric expression levels are lower than that in intestinal biopsies, reflected in the intensity of the specific gel bands corresponding to PCR product (i).
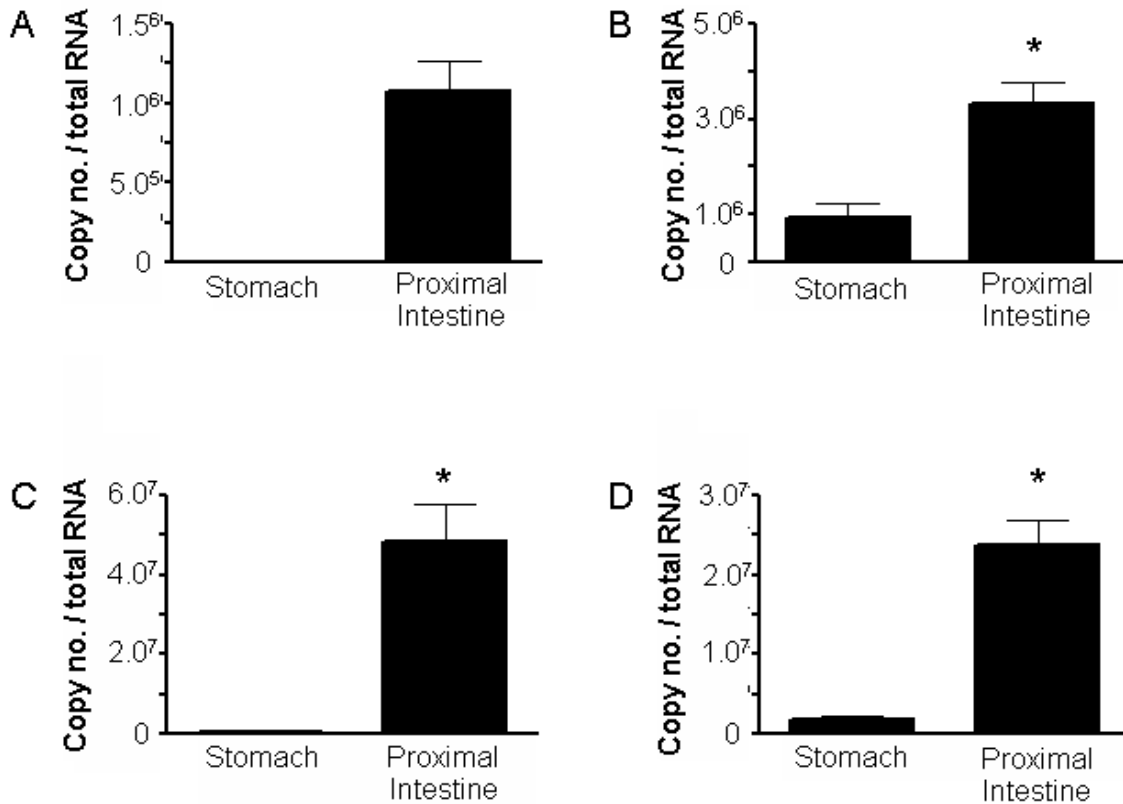
Figure 6.6.6 Comparison of expression of taste molecules in the gastric and intestinal mucosa. Absolute transcript levels of T1R2 (A), T1R3 (B), $G\alpha_{gust}$ (C) and TRPM5 (D) in the gastric and intestinal mucosa were compared. T1R2 (A) was detected in the small intestine but was absent from the gastric mucosa. T1R3 transcript levels were significantly higher in the mucosa of the intestine ($p < 0.01$) with levels 3.6 ± 0.8 fold higher than in stomach (B). $G\alpha_{gust}$ transcript levels were 70.3 ± 1.8 fold more abundant in the proximal intestine than in stomach ($p < 0.001$) (C). TRPM5 transcript levels were 13.1 ± 1.6 fold higher in the proximal intestine compared to stomach ($p < 0.001$) (D). N = 6, Mean $\pm$ SEM.

6.6.3 Gα_{gust} immunoreactivity in individual epithelial cells of the human duodenum

Slide sections of four duodenal biopsies from two patients were immunolabelled with a primary antibody directed against Gα_{gust}. Limited numbers of singularly dispersed Gα_{gust} immunopositive cells were identified amongst epithelial cells of the duodenal villi and on occasion, in the duodenal glands (Figure 6.6.7A), suggesting a restricted population of cells. No cells were observed in negative control sections where the primary antibody was omitted from the incubation (Figure 6.6.7B). Immunolabelled cells were of the open cell type (with the apical tip accessible to the lumen), and generally showed a homogenous distribution of label throughout the cytoplasm.

Immunohistochemical assays with 5-HT primary antibody showed 5-HT immunoreactivity in singly dispersed cells in the villous and glandular epithelium. Immunoreactivity in these cells was often concentrated in the basolateral half of the cell and cells appeared to be of the open cell type. 5-HT-expressing epithelial cells were more frequent in number than those expressing Gα_{gust}. In dual label assays for 5-HT and Gα_{gust} in duodenal biopsy sections there was no evidence of colocalisation within the same cells (Figure 6.6.8).

Immunolabelling for GLP-1 was observed within a limited population of singularly distributed, open type epithelial cells in the human duodenum and in fewer cells than those labelled with 5-HT. GLP-1 immunoreactivity was generally concentrated in the basal portion of positive cells. In dual label assays immunoreactivity for Gα_{gust} and GLP-1 was generally located within separate cell populations (Figure 6.6.9), however extremely rare epithelial cells showing colabelling for both markers were identified (Figure 6.6.10). However the sample size here is too small to be able to draw any definite conclusions about these cell populations and additional studies will be needed.
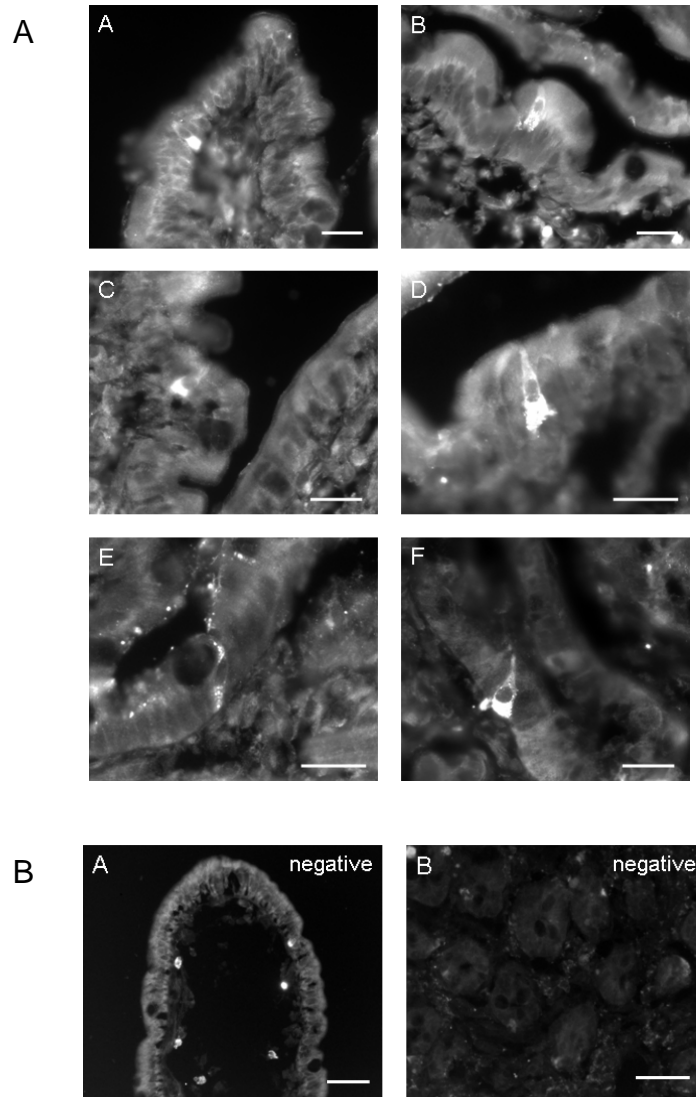
Figure 6.6.7 Gα$_{gust}$ immunoreactive epithelial cells in the human duodenum.
A: Immunolabelling for Gα$_{gust}$ was detected in the cytoplasm of singly dispersed epithelial cells in the mucosa of human duodenal biopsies. Rare Gα$_{gust}$ immunopositive cells were observed in the villous epithelium (A-E) and in the villous crypt region (F) and on occasion within the duodenal Brunner's glands. Scale bars = 50µm.
B: Negative control sections where the primary antibody was omitted from the incubation contained no positive cells either in the villous epithelium (A) or the glandular epithelium (B).
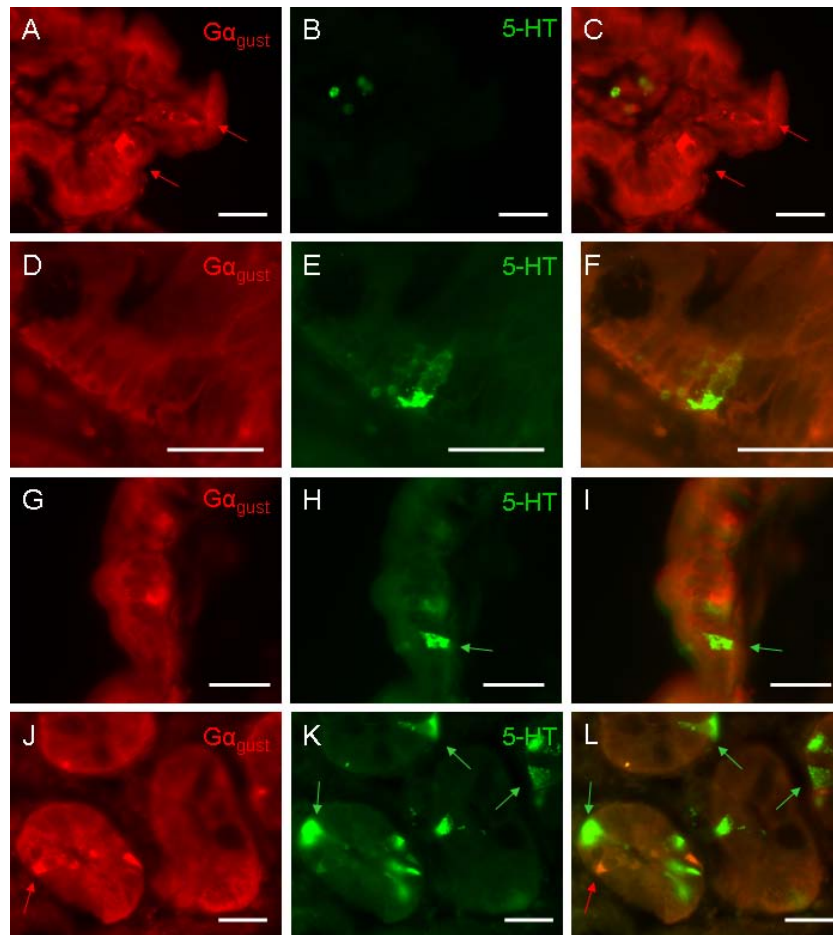
Figure 6.6.8 Gα_{gust} and 5-HT immunoreactivity in distinct cell populations in the human duodenum.
Gα$_{gust}$ and 5-HT immunoreactivity was contained within individual scattered epithelial cells in sections of the duodenal mucosa from human biopsies. Double label assays did not reveal any cells in the villous epithelium which appeared to be immunopositive for Gα$_{gust}$ (red fluorescence, A, D, G) and 5-HT (green fluorescence, B, E, H), confirmed in composite images (C, F, I) with all cells positive for only one of the two antigens. In sections where both antibodies labelled cells in the duodenal glands there was again no colocalisation between Gα$_{gust}$ (red arrow, J) and 5-HT (green arrows, K) immunoreactivities (overlay L). 5-HT immunoreactive cells were more frequent than Gα$_{gust}$ labelled cells human duodenal sections. Scale bars = 50μm.
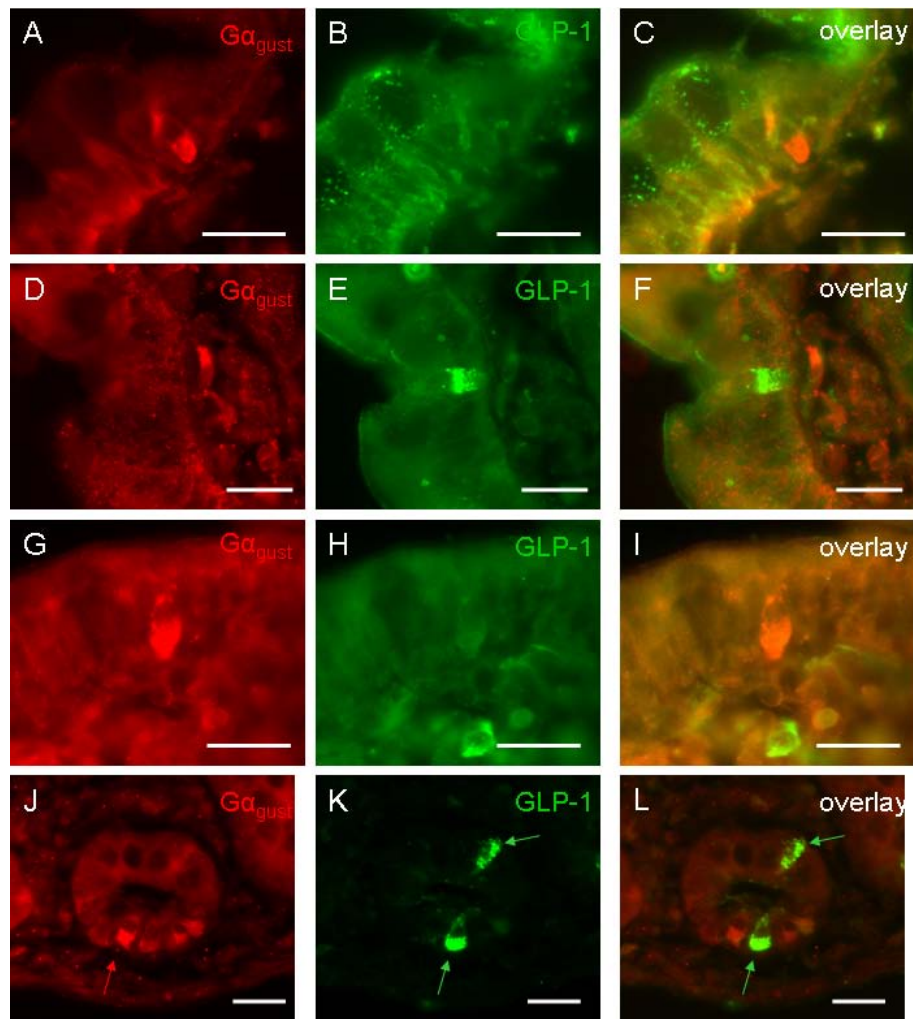
Figure 6.6.9 Gα$_{gust}$ and GLP-1 immunoreactivity in epithelial cells of the human duodenum.
GLP-1 immunoreactivity was observed within individual epithelial cells in the duodenal epithelium. Individual cells containing immunoreactivity for Gα$_{gust}$ (red fluorescence A, G) did not appear to be immunoreactive for GLP-1 (green fluorescence, B, H). Lack of colocalisation was confirmed in composite images (C, I). GLP-1 immunopositive cells (E) similarly did not coexpress Gα$_{gust}$ (D), overlay (F). Immunoreactivites of each primary antibody contained in separate cell populations shown within a villus cross-section (L).
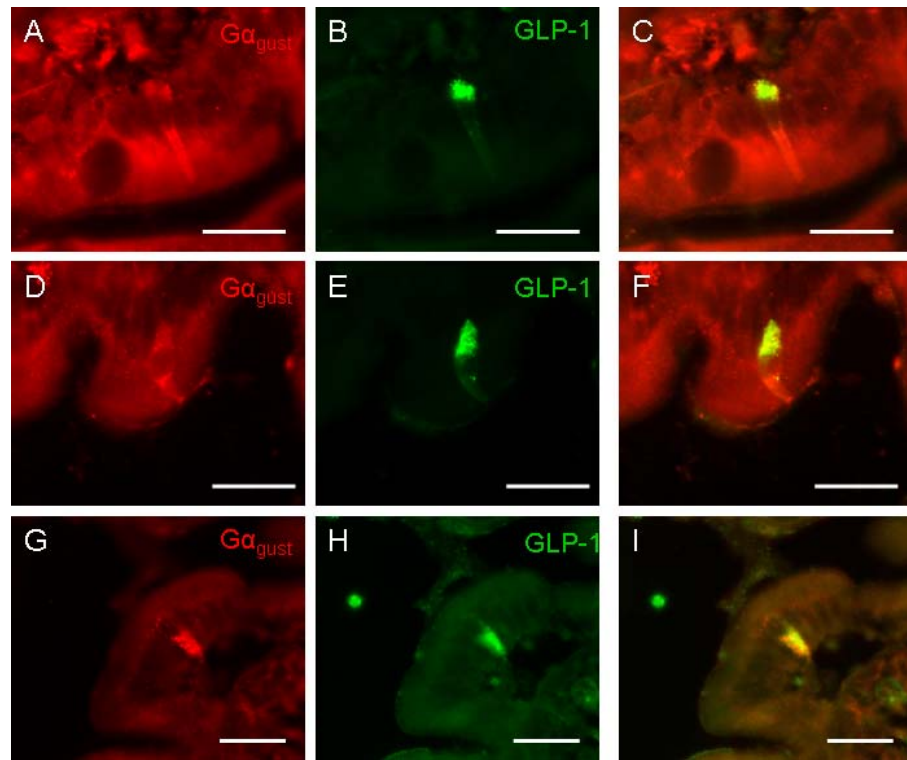
Figure 6.6.10 Gα_{gust} and GLP-1 immunoreactivity within single epithelial cells of the human duodenum
Although Gα_{gust} immunoreactive cells did not generally appear to contain any GLP-1 immunoreactivity some rare examples of apparent colocalisation were observed. Gα_{gust} immunopositive cells (red fluorescence A, D, G) appear to display immunoreactivity for GLP-1 (green fluorescence B, E, H) which is predominantly expressed in the basal portion of the cell. Composite images (yellow fluorescence C, F, I) confirm co-expression within the same cellular structures. These three examples amount to the total observations of such cells found in dual label assays from two biopsies. Scale bars = 50μm.

6.6.4 Expression of taste molecules in the duodenum in type 2 diabetes

Absolute copy numbers of each taste transcript in the duodenum was compared between patients with and without type 2 diabetes. Levels of taste molecule transcripts in the duodenum of diabetic patients, as a group, did not differ significantly from those in the duodenum of patients without diabetes (Figure 6.6.11) although the diabetic group showed more variable expression levels.

Taste molecule expression levels within the type 2 diabetic group did not correlate with age, gender, body mass index, duration of diabetes, or glycated haemoglobin. In contrast, taste molecule expression in type 2 patients showed a significant inverse correlation with the blood glucose concentration at the time of endoscopy (Figure 6.6.12) indicating that expression of taste molecules was reduced in patients with higher fasting blood glucose concentrations. This relationship was apparent for T1R2 (Spearman $r = -0.8571$, $p < 0.05$), T1R3 ($r = -0.8571$, $p < 0.05$) and TRPM5 ($r = -0.9286$, $p < 0.01$). Blood glucose concentrations were not available for the non-diabetic patients so any relationship with taste molecule expression in this group was not able to be investigated.
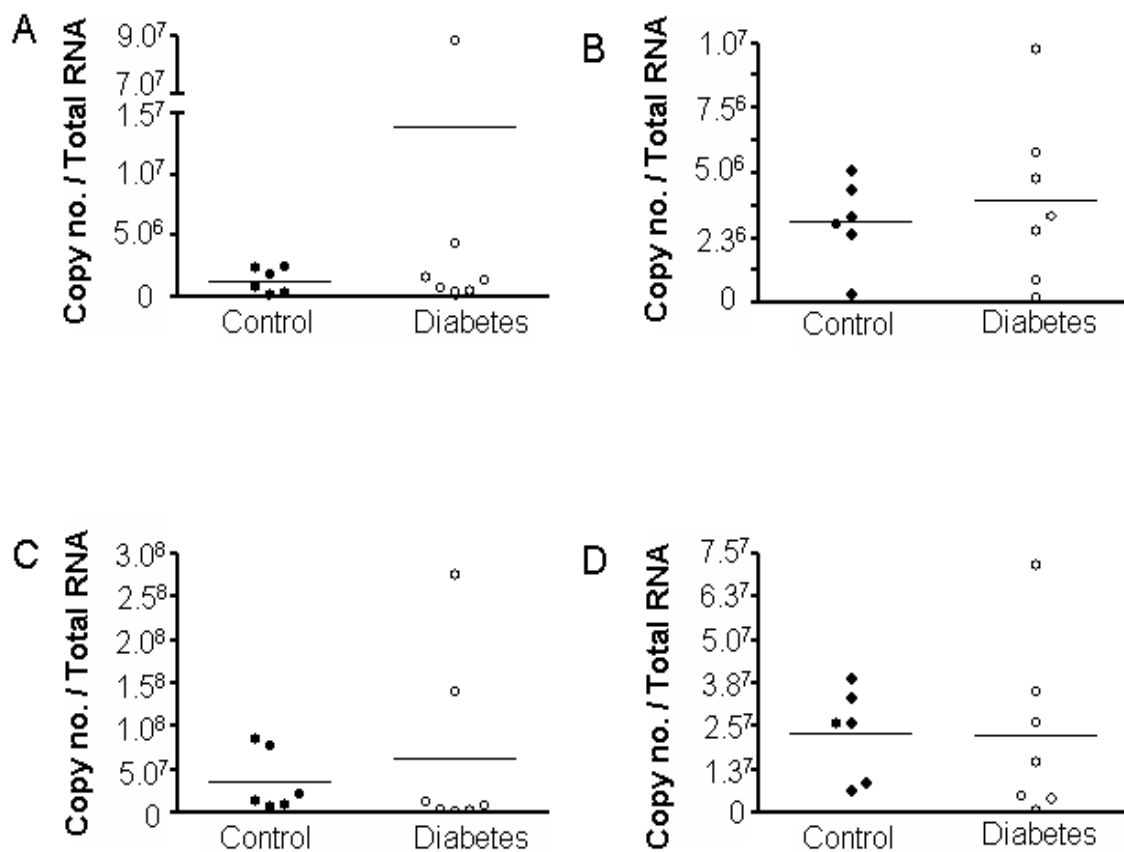
Figure 6.6.11 Expression levels of taste molecules in the duodenum are not altered in type 2 diabetic patients.
Absolute transcript levels of T1R2 (A), T1R3 (B), $G\alpha_{gust}$ (C) and TRPM5 (D) in human duodenal biopsies were compared between control subjects (filled circles) and type 2 diabetic patients (open circles). There was no significant difference in expression levels of any of the four taste molecules between the two groups. Mean ± SEM.
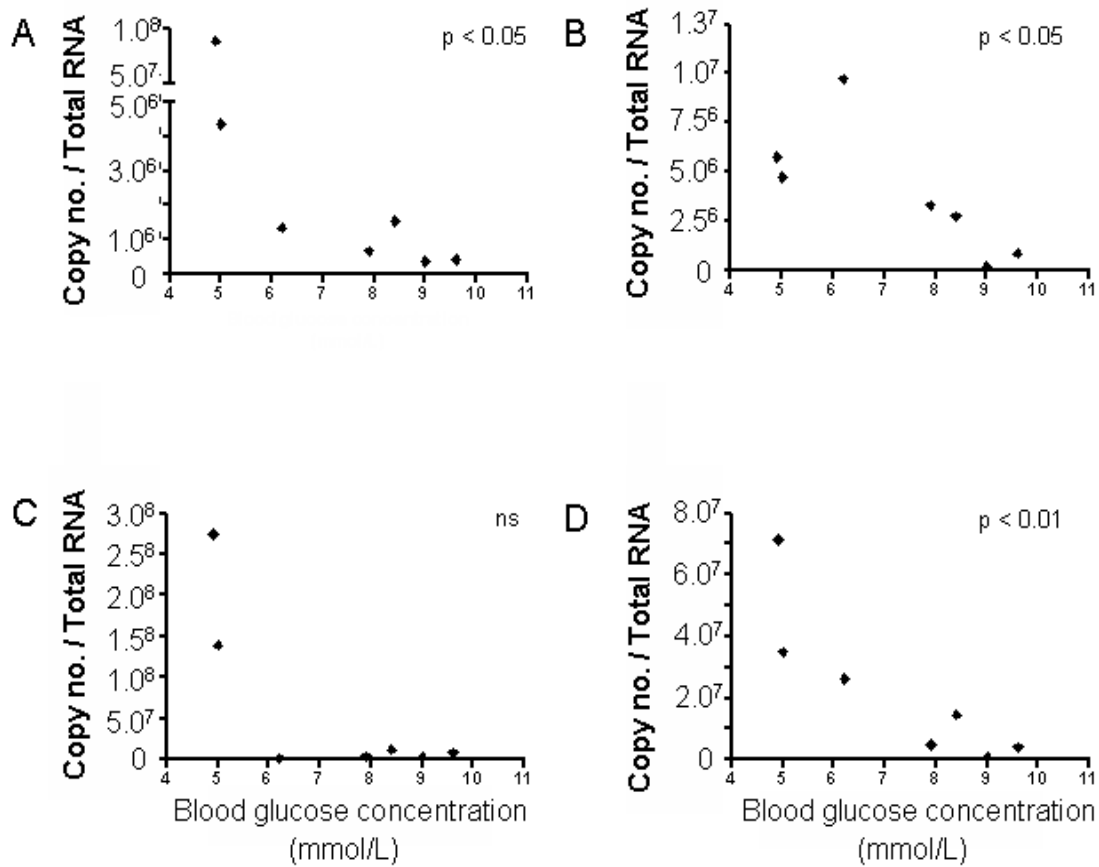
Figure 6.6.12 Taste transcript levels in the human duodenum are related to blood glucose concentration in type 2 diabetic patients.
Correlation of T1R2 (A), T1R3 (B), Gα_{gust} (C) and TRPM5 (D) transcript levels in human duodenum with blood glucose concentration. Expression of T1R2
(Spearman r = -0.8571, P < 0.05), T1R3 (r = -0.8571, P < 0.05) and TRPM5 (r = -0.9286, P < 0.01) was reduced in type 2 diabetic patients with increased blood glucose concentrations. ns = not significant

6.7 Discussion

These studies have established that taste molecules T1R2, T1R3, Gα_{gust} and TRPM5 are specifically expressed in the upper gastrointestinal mucosa in humans, strongly supporting the concept that a sweet taste pathway, similar to the tongue exists in the gut. Quantification of absolute mRNA copy numbers of each taste molecule showed substantial regional specialisation, with predominant expression in the proximal small intestine, a key site for nutrient detection. These taste molecules are, therefore, likely to represent at least one type of sensory apparatus for detection of luminal sugars. Furthermore the observation that the expression of T1R2, T1R3 and TRPM5 is inversely related to the blood concentration of glucose in type 2 diabetic patients, suggests that the signalling of nutrient from the gut lumen is under dynamic metabolic control.

All taste molecules were predominantly expressed in the mucosa of the proximal intestine compared to the stomach. Indeed the sweet taste specific receptor T1R2 was exclusively expressed in the small intestine, establishing that a sweet taste pathway does not operate in the stomach. This expression also occurs at a site relevant to the triggering of signals that regulate absorption, slow gastric emptying, suppress appetite and cause sensations such as fullness in response to carbohydrates (82, 106, 124, 215, 216, 274). The differences in human expression of taste molecules in gastric and proximal small intestine regions are therefore consistent with the different roles of these gut regions in the processing of ingested material.

Quantitative expression data in the human intestinal mucosa show that Gα_{gust} and TRPM5 transcripts were present at higher levels than transcripts for T1R2 and T1R3. In comparison to taste transduction on the tongue this stoichiometry of expression may fit with what is known about chemoreception of different taste modalities. On the tongue, T2R and T1R receptors are expressed in mutually exclusive populations of taste cells with the T1R cell population subdivided into those that express a T1R2 + T1R3 heterodimer and

function as broadly-tuned sweet taste cells, and those that express a T1R1 + T1R3 heterodimer and function as *umami* taste cells (1, 237). All three cell types share a common $G\alpha_{gust}$ / TRPM5 signalling pathway (377). As a consequence, the higher copy number of $G\alpha_{gust}$ and TRPM5 transcripts in the proximal intestine may reflect their additional expression in bitter-taste cells (366), or differences in post-transcriptional processing of molecules involved in taste transduction.

An intriguing outcome of this molecular study was the identification of high expression levels of T1R3 transcripts in the distal esophagus, in the general absence of other taste molecule transcripts. This comparatively high level expression of T1R3 in the esophagus was also noted in the mouse gastrointestinal tract (Chapter Two). In both species, T1R2 expression was absent from this region, suggesting that esophageal T1R3 is not involved in carbohydrate detection. Expression of T1R1 was not assessed in these studies so it is conceivable that T1R1 + T1R3 heterodimers in the distal esophagus might function as an L-amino acid sensor, as they do in the tongue, with potential role(s) in sensing of refluxed gastric material. Regional expression data from the upper gastrointestinal tract in mouse and humans were similar in regards to T1R2 and T1R3 expression levels. There were however differences between humans and mice in $G\alpha_{gust}$ and TRPM5 expression. $G\alpha_{gust}$ transcript levels in mice were most abundant in the gastric antrum followed by the ileum and the gastic antrum was also a predominant region of TRPM5 expression. Whereas in humans the expression profile of these transcripts was similar to that of the T1R receptors with expression largely specific to the proximal small intestine, indicating that there are some species differences in expression of taste molecules in the gastrointestinal tract.

Similar to results in the mouse small intestine and human colon, $G\alpha_{gust}$ immunoreactivity was identified in single dispersed epithelial cells in duodenal biopsies (294). $G\alpha_{gust}$ immunopositive cells were infrequent in the human duodenal biopsies assessed by immunolabelling, indicating they represented a limited

population of the total pool of epithelial cells within the biopsy tissue, indicating perhaps that this will not prove to be the only nutrient sensing mechanism in operation. Studies in the mouse small intestine (Chapter Three) have established that $G\alpha_{gust}$ expressing cells are preferentially located in the jejunum compared to duodenum; whether this is also the case in humans will require further studies.

Double label assays with $G\alpha_{gust}$ and 5-HT in humans did not reveal any cells that coexpressed both markers. However a population of cells in mice that did coexpress was identified within the jejunum, where $G\alpha_{gust}$ positive cells were most frequent. Whether this holds true in humans would require comparison in human jejunal biopsies, and would be be technically difficult to access. In a similar manner to 5-HT results, dual immunolabelling for GLP-1 and $G\alpha_{gust}$ in human duodenal biopsies did not reveal a distinct colabelled population. Again, dual labelled intestinal cells for GLP-1 and $G\alpha_{gust}$ in mice were mostly observed in the jejunum where $G\alpha_{gust}$ immunopositive cells predominated; whether this is a reflection of regional expression patterns would require a more comprehensive immunohistochemical study with human tissue. However rare examples of cells that contained both $G\alpha_{gust}$ and GLP-1 were observed. $G\alpha_{gust}$-expressing cells identified by immunohistochemistry in the human colon have also been reported to coexpress immunoreactivity for GLP-1 and peptide YY (294). In the current study, however, too few $G\alpha_{gust}$ immunolabelled cells were identified from too few human intestinal biopsies to be able to accurately determine whether the brush cell-predominant phenotype of $G\alpha_{gust}$ cell populations in the mouse intestine is conserved in the human gastrointestinal tract. It is known that in the human colon $G\alpha_{gust}$ immunoreactivity does not colocalise with the brush cell marker villin which has been reported to indicate that these are not brush cells (294), however this is not the best marker to show this. Indeed, knowledge of human gastrointestinal brush cells is limited and no species-specific lectin markers are known (102). Respiratory brush cell numbers are reported to be less frequent in humans than in rodents (279), and recent information on ultrastructurally identified duodenal brush cells has reported only 6 positively identified cells from over 300 human intestinal biopsies (228). This

indicates that few brush cells are likely to exist in the human gastrointestinal tract. Even though $G\alpha_{gust}$ immunopositive cells identified in this study were infrequent, they were detected in each of the duodenal biopsies processed for immunohistochemistry indicating that they are likely to represent a larger pool of cells than that presumed for human duodenal brush cells and therefore it is unlikely that these two cell types are fully coincident.

Despite the finding that key taste molecules are present in the upper gastrointestinal tract of humans, it is yet to be precisely determined how nutrient sensing mechanisms operate, the mediators released and nerve pathways activated by taste cells. The current preliminary immunohistochemical investigations reveal that taste cells in the human duodenum do not release 5-HT and that very few have the capacity to release GLP-1. This suggests that taste transduction in the human intestine may involve the release of alternative mediators. A recent study has reported that human duodenal L cells express $G\alpha_{gust}$ (159) and that stimulation of the human enteroendocrine L cell line NCI-H17 with sugars leads to GLP-1 release, a response that is blocked by a T1R3 receptor antagonist. Immunohistochemical cell counts in this study reported that 90% of L cells express $G\alpha_{gust}$ in duodenal biopsies obtained from cadavers. This number appears to be in contrast to the observations in the current study despite the same antibodies being used in both. This descrepancy may arise from the differences in tissue sources of fresh and post-mortem biopsies. However $G\alpha_{gust}$ cell counts of Jang and colleagues indicate that there is a significant population of $G\alpha_{gust}$ expressing cells which do not contain GLP-1 or GIP supportive of alternate mediators existing in intestinal taste cells.

Expression of intestinal taste molecules in patients with or without type 2 diabetes did not reveal any group differences in transcript levels. However care must be take in interpreting this finding as evidence of a lack of adaptation of taste molecules in type 2 diabetes as studies have shown that mRNA levels may not always reflect protein abundance (114) and differential post-transcriptional regulation of taste molecules

may occur in these patient groups. A limitation of this study when comparing patients with and without type 2 diabetes is the low number of samples in each group; greater numbers and stratification of diabetics into different groups, including type 1 diabetes, would allow a more complete picture of potential changes.

This study has provided novel evidence that taste molecule expression is modulated according to the metabolic profile in type 2 diabetic patients. Specifically, expression of taste molecule transcripts for T1R2, T1R3 and TRPM5 in the duodenum of these patients was inversely correlated with the blood glucose concentration at the time of tissue sampling. $G\alpha_{gust}$ transcript levels in type 2 diabetic patients did not show a statistically significant correlation, however, the patients with the highest copy number of $G\alpha_{gust}$ transcript had the lowest blood glucose levels. However subsequent to these analyses additional duodenal biopsies have been collected and with double the number of diabetic patients the correlation with blood glucose levels has only been strengthed and is significant across all four taste molecules. Because intestinal taste molecule expression did not significantly correlate with glycated hemoglobin, a longer-term marker of glycemic control, it appears that mucosal expression of taste molecules is dynamically regulated at the transcriptional level in direct response to blood glucose concentrations. Indeed, the lack of group differences in the expression of taste molecules in patients with and without type 2 diabetes may reflect the relatively modest range of blood glucose concentrations in these type 2 diabetic patients, which were in the normal postprandial range.

Acute variations in the blood glucose concentration, even within the physiological postprandial range, are known to modify gastrointestinal motility and slow gastric emptying in both diabetic patients and healthy volunteers (13, 96, 97, 114, 202). Such regulation of gastric emptying in a high glycemic state would have the beneficial effect of delaying further entry of carbohydrate into the small intestine, thereby preventing further increases in blood glucose. The decrease in taste molecule expression seen here in hyperglycemia

may form part of another compensatory mechanism to avoid further increases in blood glucose levels by limiting small intestinal absorption. Although the time lag from transcription to changes in protein levels would have to be investigated to elucidate when functional changes could be expected to take effect. It is well recognised that glucose is transported from the intestinal lumen via the glucose transporters SGLT1 and GLUT2. Taste receptors T1R2 and T1R3 have been shown to be coupled to the up-regulation and apical insertion of these transporters in intestinal epithelial cells, to increase the absorptive capacity in the presence of luminal carbohydrate (201, 203). A short-term downregulation of taste receptors would therefore tend to diminish the capacity for glucose-induced upregulation of transporters and further reduce absorption of glucose when the blood concentration is inappropriately high, especially as glucose transporters in the epithelium of type 2 diabetes are reported to have increased expression compared to healthy controls (83). Equally, it is tempting to speculate that the increased expression of intestinal sweet taste molecules observed in fasted mice (Chapter Five) reflects a mechanism to upregulate glucose transport capacity in rapid response to the re-appearance of glucose following a prolonged fast. Whether systemic and/or intestinal signals contribute to this regulation and in what proportions will require further exploration. Potentially the transcription of taste molecules in the small intestine may be regulated by both luminal and systemic signals. However the correlation between intestinal taste molecule expression and blood glucose concentration described in the current study, does not establish causation; to do this, a separate study would be need to be performed involving a glucose clamp technique.

In conclusion, this study has established that taste molecules show region-specific expression in the human gut and that their expression is inversely regulated according to blood glucose concentration in type 2 diabetic patients with hyperglycaemia although not able to investigate this relationship in controls. This not only supports the concept that the gut is able to "taste" its contents in a similar way to the tongue, but also that expression of intestinal taste receptors is under dynamic metabolic control.

7. DISCUSSION

7.1 General discussion and future experiments

Intestinal nutrients stimulate positive and negative feedback pathways to regulate feeding behaviour and gastrointestinal secretory and motor functions in order to optimise digestion and absorption of ingested meals. Feedback is likely mediated upon detection of nutrients at the apical membrane of specialised epithelial cells by activation of intracellular signalling cascades leading to basolateral membrane release of neurotransmitters and activation of receptors on sub-epithelial vagal afferents.

Satiation and the delay in gastric emptying induced by luminal carbohydrates is thought to occur via such a pathway, and involve the specific release of serotonin (5-HT), glucagon-like peptide 1 (GLP-1) or other neurotransmitters from basolateral secretory vesicles. However not all events along this pathway are clearly defined, and the molecular mechanisms through which carbohydrates are detected and 5-HT, GLP-1 or other neurotransmitters released represent a particular gap in understanding of intestinal nutrient sensing. The studies in this thesis were aimed to investigate, firstly, whether taste molecules were expressed in the intestine and could constitute the detection and transduction machinery for carbohydrate-mediated release of 5-HT, GLP-1 or other neurotransmitters. Secondly, these studies were performed to gauge whether any alteration in expression of taste molecules occurred in altered dietary and disease states that subserved adaptation of carbohydrate-induced gastric motility reflexes. These aims were investigated by anatomical and molecular assessments of four key sweet taste molecules in the small intestine of mice and humans.

The key sweet taste molecules T1R2, T1R3, $G\alpha_{gust}$ and TRPM5 were identified in the mucosa of both the

mouse and human gastrointestinal tract, and showed preferential expression in the proximal small intestine in both species. This expression is consistent with the presence of sweet taste machinery within the intestinal region responsible for initiation of carbohydrate-sensitive reflexes that delay gastric emptying and inhibit food intake. Furthermore taste molecule expression was largely absent from the stomach, consistent with the different roles of these gut regions in the processing of ingested material. Therefore it is likely that the small intestine is able to identify chemical stimuli through a transduction mechanism similar to the tongue. However precisely how intestinal 'taste' cells are able to signal this information remains unclear.

Interestingly both humans and mice had high expression levels of T1R3 in the mucosa of the distal esophagus, in the absence, or very low abundance, of other taste molecule transcripts. In the absence of co-expression of the sweet-taste specific T1R2, expression of T1R3 is unlikely to represent a sweet sensing mechanism in the esophagus, rather, if expressed with the T1R1 receptor it may constitute a *umami* or L-amino acid sensor of refluxate or ingested amino acids. Humans and mice, however, differed in their expression of taste molecules in the gastric antrum - in humans taste transcript levels were low and equivalent to other gastric regions, however peak levels of $G\alpha_{gust}$ and TRPM5 transcripts were found in the mouse antrum and may reflect different regional roles of specific taste pathways between species. Indeed large clusters of $G\alpha_{gust}$-expressing cells have previously been identified beyond the fundus around the limiting ridge of the mouse stomach (117). $G\alpha_{gust}$ and TRPM5 in the mouse stomach do not signal the presence of sugars because the sweet receptor T1R2 is absent, but have been shown to couple to T2R receptors to signal bitter stimuli (366). The mouse stomach may therefore have a greater capacity to detect bitter compounds than that of humans. This may have direct relevance for mice where the early recognition of potentially harmful compounds is critical as they lack the ability to regurgitate. Bitter detection in the stomach may then stimulate compensatory reflexes such as excess mucous secretion and pica behaviour (343). The longitudinal expression patterns of taste molecules observed in these studies in humans and

mice have since been supported by findings of other studies now published (20, 81).

Immunohistochemical studies performed in mice localised expression of three taste proteins, T1R3, $G\gamma_{13}$ and most comprehensively $G\alpha_{gust}$, to individual epithelial cells most frequently observed in the upper villous region, confirming the existence of intestinal 'taste' cells. Although this study was able to show that individual epithelial cells were immunopositive for these taste proteins all three antibodies were raised in rabbits, precluding double label assays by traditional indirect immunofluorescence methods. This prevented direct demonstration of multiple taste proteins within the same cellular structures and thus whether a complete taste signalling cascade may be present. A recent study has overcome this problem by using intestinal tissue from transgenic mice expressing enhanced green fluorescent protein under the control of the TRPM5 promoter which allowed immunolabelling of other taste proteins on the same sections (20). The results of Bezençon and colleagues (20) indicate that solitary taste cells do express multiple taste proteins, however colocalisation patterns show regional variations. In the small intestinal villi of mice expression of TRPM5 largely colocalised with $G\alpha_{gust}$, T1R1 and T1R3 but not PLCβ2. However TRPM5 cells in the glandular epithelium in this region showed a reduced degree of colocalisation with other taste proteins. Similarly TRPM5 cells in the colon showed a high degree of colocalisation with $G\alpha_{gust}$ but not PLCβ2 or T1R1, while T1R3 was not identified. This suggests that intestinal taste cells are a heterogeneous population, not only tuned to detection of different chemical stimuli through the expression of specific receptors but may use different downstream transduction pathways to effect release of different mediators and thereby, to regulate multiple gastrointestinal functions. Therefore there may be multiple types of 'taste' cells in the gut.

Bezençon and colleagues (20) did not detect T1R2 immunoreactivity in any region of the mouse gastrointestinal tract. Recently available commercially produced T1R2 antibody was assessed in both

mouse and human intestinal tissue by immunohistochemistry within the current studies and no convincing labelling was observed (data not shown). The lack of positive immunolabelling in taste buds in control sections from the mouse tongue suggests that this is not a high quality or specific antibody for the detection of T1R2 in tissue sections. Dyer *et al* (81) have reported T1R2 protein expression in the mouse small intestine using western blot although published images indicate a very low signal. In an RT-PCR study by Bezençon and colleagues (20) it was reported that T1R2 was present at detectable levels only in the mouse ileum, and was barely detectable in the human GI tract. In contrast, the current studies have shown that while T1R2 is a low abundance transcript in human and mouse intestine, it is expressed in all regions with predominance in the proximal small intestine. Comparable T1R2 expression has been independently demonstrated in all regions of the mouse small intestine by others using real time RT-PCR (81). Varying T1R2 levels reported by different research groups are likely to relate to methodological differences that reflect the relative sensitivities of the assays used, as T1R2 is weakly expressed in whole mucosal intestine tissue. However, low level expression of T1R2 in whole mucosal tissue may not reflect T1R2 protein levels in individual sweet sensing cells. From knowledge of lingual taste transduction it is widely accepted that different taste compounds are detected by modality specific taste receptor cells which express only the receptors for those tastants (237, 377). Therefore only small subsets of intestinal taste cells are likely to be specifically tuned to detect sugars. Within this cell population expression levels of T1R2 are likely to be high but diluted by larger cell populations in a whole mucosal sample. Knowledge of which intestinal taste cells are capable of detecting sugars, and which transduction pathways they employ would be extremely valuble and an important focus for future studies. As antibodies for T1R2 are suboptimal for immunohistochemical coexpression studies, investigations focussed on which other taste proteins are specifically expressed in intestinal sweet sensing cells must be studied by other methods. Immunofluorescence *in situ* hybridisation has been successfully used to detect taste receptors in tongue sections (142, 172, 223, 237) and may be used to determine which downstream taste transduction molecules are coexpressed in intestinal T1R2 cells

and if their expression differs in intestinal regions. The identification of unique signalling molecules in intestinal sweet taste cells has the potential to identify new targets for drug design that may alter carbohydrate-mediated intestinal feedback, which may benefit patients with diabetes mellitus and/or obesity.

A key question investigated in these studies was whether a $G\alpha_{gust}$-dependent taste pathway may be the unknown transduction mechanism linking the presence of intestinal carbohydrate to 5-HT and GLP-1 release from the epithelium. Colocalisation studies in the mouse small intestine revealed a subpopulation of $G\alpha_{gust}$ expressing cells that coexpressed 5-HT and GLP-1, however this cell phenotype was a minority compared to individual $G\alpha_{gust}$ and enteroendocrine cell populations in the jejunum. This suggests that intestinal 5-HT and GLP-1 release can occur via both $G\alpha_{gust}$-dependent and $G\alpha_{gust}$-independent mechanisms. However the majority of $G\alpha_{gust}$-expressing cells as yet do not have an identifable signal transmitter and the impact of $G\alpha_{gust}$ on 5-HT and GLP-1 release will have to be studied functionally. These potential pathways of nutrient signalling in the gastrointestinal mucosa are summarised in Figure 7.7.1.

$G\alpha_{gust}$-independent mechanisms of glucose detection in enteroendocrine cells have been described in a GLP-1 secreting cell line, GLUTag, where glucose metabolism leads to cellular depolarisation through closure of K_{ATP} channels, which trigger GLP-1 release (280). Further support for the well characterised pancreatic β-cell glucose-sensing mechanism has been provided by RT-PCR in GLUTag cells which has confirmed expression of three key molecules of this pathway SUR1, $Kir_{6.2}$ and glucokinase (280). However glucose-stimulated GLP-1 release can also occur from GLUTag cells via a second mechanism independent of glucose metabolism, in which GLP-1 release can be blocked by inhibitors of the sodium-glucose co-transporters SGLT-1 and SGLT-3 expressed by these cells (111). Additionally in another GLP-1 secreting cell line, NCI-H716, a T1R3 receptor antagonist blocks secretion (159). In a similar manner in BON cells, a

human 5-HT-secreting cell line which expresses SGLT-1, glucose-mediated release of 5-HT can be blocked

by phloridzin, a potent SGLT inhibitor (170). There is the potential for multiple transduction mechanisms to

exist within the same cell or within enteroendocrine cell subtypes. Importantly however, these responses

have yet to be demonstrated in native enterochromaffin or L-cells *in vivo*. The endocrine cell lines used to

study the mechanisms of gut hormone secretion *in vitro* differ significantly from native enteroendocrine cells.

STC-1 cells, for example, express an array of hormones in contrast to native enteroendocrine cells which

have one major secretory product. Moreover, STC-1 cells are non-polarised in culture suggesting that

caution should be used in extrapolating cell culture results to sensory mechanisms acting in

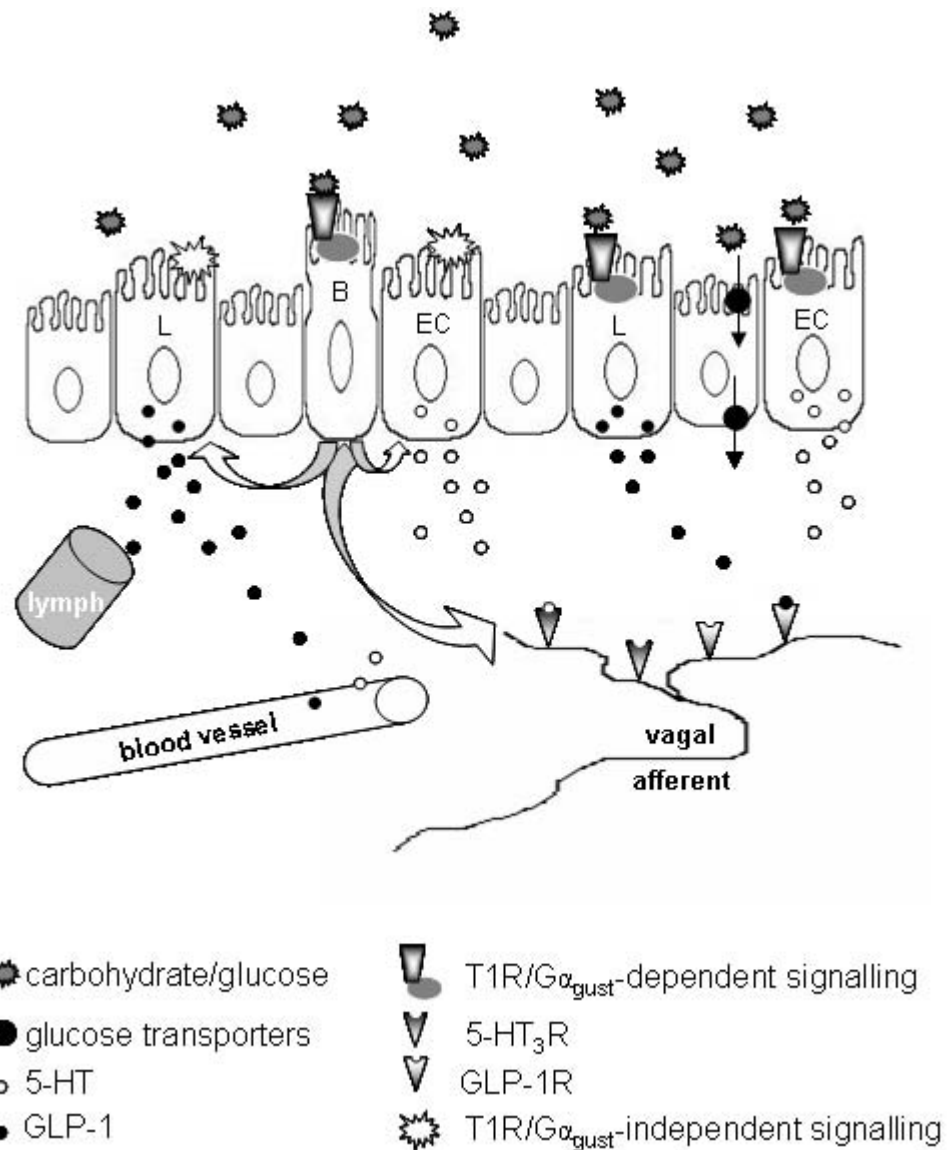enteroendocrine cells *in vivo* (31).

Figure 7.1.1 Potential carbohydrate sensing pathways in the small intestinal mucosa.
Postulated pathways in the signalling of luminal carbohydrates as investigated and reviewed in this thesis
are illustrated. Chemosensory pathways are likely to be complex and involve multiple primary
chemosensory cells. Taste transduction mechanisms, indentified by expression of $G\alpha_{gust}$, exist in a subset
of enterochromaffin (EC) and L cells suggesting that $G\alpha_{gust}$-depedent signalling of the presence of luminal
carbohydrate may occur in these cells and lead to 5-HT and GLP-1 release, allowing entry to the lymph,
blood vessels and in particular activation of receptors on vagal afferents. Release of 5-HT and GLP-1 may
additionally occur through $G\alpha_{gust}$-indepedent signalling pathways as not all cells in these populations are
equipped to 'taste' the luminal contents. Brush cells (B) are also equipped to transduce carbohydrate signal
via an $G\alpha_{gust}$-depedent mechanism and the subsequent release of as yet unknown messenger (potentially
gaseous) may transfer this signal to nearby enteroendocrine cells promoting vesicular excytosis or directly
act on vagal afferents.

Further characterisation of the human sodium-glucose transporter family has revealed that SGLT-3 does not function as a transporter but as a glucose sensor by binding glucose and causing membrane depolarisation in cell expression systems (76). In yeast many homologues of glucose transporters have been identified which do not have detectable transporter activity but act as glucose receptors (138). The human SGLT-3 protein is expressed in skeletal muscle and in the small intestine where it is found in cholinergic neurons of the enteric nerve plexuses; however it is not expressed in human enterocytes like SGLT-1. Although the putative role of SGLT-3 as a glucose sensor has not been confirmed in rodent species, the expression of SGLT-3 has been recently identified in the rat duodenal mucosa by Freeman and colleagues (98). These authors suggested that due to a lower affinity of SGLT-3 for glucose compared to SGLT-1, the high concentrations of glucose needed to stimulate 5-HT release from BON cells may reflect an action at SGLT-3 rather than SGLT-1 transporters. However SGLT-3 expression has not yet been demonstrated in native enterochromaffin cells, and studies using in vitro models of glucose-stimulated 5-HT and GLP-1 secretion have shown that release is attenuated by the SGLT blocker phloridzin, which in vivo does not inhibit glucose-induced slowing of gastric emptying in rat (271). In summary, SGLT transporters may contribute to reflex slowing of gastric emptying due to their important roles in glucose binding and transport however a direct role in glucose sensing will require further investigation.

The presence of a unique population of $G\alpha_{gust}$ immunopositive cells in the mouse jejunum which coexpress 5-HT or GLP-1 suggest that the roles of these hormones as 'taste' mediators is confined to this region in mice. In the human gastrointestinal tract $G\alpha_{gust}$ immunopositive cells that coexpress GLP-1 have also been identified in the colon (294) as well as duodenum (160) indicating there may be significant species and regional differences. Using post-mortem duodenal tissue, Jang and colleagues (160), reported that over 90% of L-cells contained $G\alpha_{gust}$ and have confirmed expression by RT-PCR in laser captured L-cells. These results differ to the duodenal immunolabelling results from the current study, where the overwhelming

majority of Gα_{gust} and GLP-1 immunolabelling was present within separate cell populations, with only rare examples of Gα_{gust} positive L-cells. Cell counts of Gα_{gust} expressing cells in the study of Jang and colleagues (160), however, show that fewer than 50% of Gα_{gust}-expressing cells in human duodenum were L-cells and therefore other mediators of taste signaling are likely to exist in human Gα_{gust} cells. Differences in cell populations identified between this and the current studies may be due to methodological issues such as tissue source, however due to the limited number of human duodenal samples assessed in the current study it will be important to confirm results in additional biopsies. Moreover, it will be important to establish which other epithelial cell types express Gα_{gust} in humans.

The Gα_{gust} cell populations that separately coexpressed 5-HT or GLP-1 in the mouse small intestine may be tuned to subserve specific nutrient-evoked gastrointestinal reflexes. Recent functional experiments performed in mice deficient in Gα_{gust} show that they have profoundly reduced GLP-1 release *in vitro* and *in vivo* in response to glucose (160). This provides the first direct evidence that sweet taste mechanisms are functionally active and linked to GLP-1 secretion in response to luminal carbohydrate in mice. It remains to be revealed what other epithelial cell types and mediators are functionally important in sweet taste signalling.

Gastrointestinal Gα_{gust}-cells were originally identified as brush cells in the rat stomach and duodenum based on immunolabelling for cytoskeletal markers (137). The current studies have extended this finding, and shown that brush cells (which bind the lectin UEA-1 in mice) are also the major phenotype of gastrointestinal Gα_{gust} cells in mice. The work of Bezençon and colleagues has also provided complementary evidence that TRPM5-expressing cells in the mouse small intestine display characteristic features of brush cell morphology (20). These authors also assessed immunoreactivity for gut peptides cholecystokinin, peptide YY, ghrelin, orexin A and GLP-1, known to be involved in food intake control, in

TRPM5-cells and failed to identify colabelling. In summary therefore, the majority of Gα_{gust}-cells in the rodent small intestine show characteristics of brush cells but small subsets within the jejunum (current study) and antrum (293) do not, and label for enteroendocrine cell markers 5-HT and GLP-1. The human respiratory and gastrointestinal tracts have fewer brush cells than equivalent regions in rodents (228, 279) and as such Gα_{gust} is likely to be present in other cell types such as enteroendocrine cells in humans. Results to date, however, have only defined a small proportion of Gα_{gust}-cells in the human intestine and these contain GLP-1 or GIP. Gα_{gust} may also be expressed in other enteroendocrine cell types such as cholecystokinin containing I-cells, as bitter stimuli has been shown to lead to CCK release from STC-1 cells (44), or in cells that release non-traditional mediators. For example, brush cells in rats have been proposed to use NO as a transmitter (179), although in the current studies immunoreactivity for nNOS was absent from the mouse jejunal epithelium. Equally, other gaseous signalling molecules may be released by taste mechanisms in the gastrointestinal tract. Recently ATP has been implicated as an important transmitter in the activation of gustatory sensory nerves in response to sweet, umami and bitter stimuli, as these are lost in mice which lack P2X$_2$ and P2X$_3$ purinergic receptors (26, 93, 165). An equivalent role for ATP as a key transmitter in gastrointestinal taste transduction remains to be investigated.

TRPM5-expressing cells in the gastrointestinal tract do not contain the presynaptic marker SNAP25 (20) indicating there are unlikely to be direct synapses between gastrointestinal taste cells and nerve fibres. This is not surprising as intestinal epithelial cells are continually renewed over 2 - 3 days as new cells emerge from the crypt and mature cells slough off from the villus tip, making direct synapses difficult to maintain. Therefore activation of mucosal vagal afferent fibres by enteroendocrine cell products is through a paracrine mechanism (18). Intestinal taste cells are likely therefore to release their mediators to activate afferent fibres by paracrine means (Figure 7.1.1). However it is also possible that intestinal taste cells may act as intermediaries in paracrine activation of other, nearby enteroendocrine cells. In such a scenario the

presence of carbohydrate may trigger T1R receptors on these primary sense cells causing basolateral release of mediators that recruit other, adjacent populations of enteroendocrine cells to release their secretory products (31, 133). This mechanism may amplify the response to carbohydrate in the intestine and could parallel the pathway of sensory nerve activation by sapid molecules described on the tongue. Here, type II taste cells containing taste molecules do not possess synapses, and use paracrine signals to activate type III taste cells, which make synaptic contact with gustatory nerves (287, 288).

Although key sweet taste molecules were identified in the upper gastrointestinal tract in the current studies, it is yet to be precisely determined which gastrointestinal feedback mechanisms are stimulated by taste signalling. Although the mediators released and nerve pathways triggered by gastrointestinal taste cells are likely to be diverse, the exact functional processes which couple to this mechanism require further investigation. A role for taste receptors in the postprandial recruitment and translocation of glucose transporters to the apical membrane has been proposed (201, 203). The facilitative glucose transporter GLUT2 is rapidly recruited to the apical membrane of enterocytes by artificial sweeteners acting at apical T1R2 and T1R3 receptors (201). Moreover, the upregulation of SGLT-1 protein that occurs in response to a high carbohydrate diet in normal mice is absent in mice deficient in either T1R3 or $G\alpha_{gust}$ (203).

Functional experiments designed to test the involvement of sweet taste molecules in gastric emptying responses to intestinal carbohydrate were not reported in this thesis. A study using mice deficient in $G\alpha_{gust}$ or TRPM5 was planned to test the rate of gastric emptying of glucose using a non-invasive C^{13}-octanoic acid breath test developed in mice (336, 337). Unfortunately these knockout mice did not breed within a timeframe suitable to complete studies for this thesis, but these remain a key experiment for the future. A further aim of these studies was to determine if GLP-1 directly activated mucosal vagal afferents in the same manner as 5-HT, or whether the action of GLP-1 on vagal afferents occurs only following absorption,

in the portal vein (231, 242, 351). Although GLP-1 was without effect on the activity of gastroesophageal afferents *in vitro*, these studies were unable to assess specific effects on intestinal vagal afferents due to methodological limitations. To assess a direct action of GLP-1 on vagal afferents using an electrophysiological approach in the future will require an *in vivo* animal approach where the mucosa is preserved.

However an anatomical approach may yield further insight into the GLP-1 signalling potential of mucosal vagal afferents. Expression of the GLP-1 receptor has been demonstrated in the rat nodose ganglion (234). Using retrograde tracing techniques developed in our laboratory vagal afferents that project to the small intestinal mucosa can be labelled in mice, enabling identification of target-relevant afferents (374). These vagal afferents can then be harvested from nodose ganglion sections by laser-capture microdissection of fluorescence-positive soma (154), subjected to RNA extraction and quantitative real time RT-PCR assessment of GLP-1 receptor transcript levels. This approach would establish if mucosal vagal afferents are specifically equipped for activation by GLP-1. Additionally retrograde tracing could be combined with immunohistochemistry to assess GLP-1 receptor protein expression.

It is well established that motor and secretory responses of the gastrointestinal tract to luminal stimuli are altered by prior nutrient intake, and in certain disease states (143, 277). This suggests that the sensory mechanisms that subserve them are capable of adaptation, which may benefit the individual, or trigger gastrointestinal dysfunction and symptoms in disease. The current studies have shown that expression of taste molecules is differentially regulated in fed and fasted mice and in humans with type 2 diabetes, leading to increased expression in fasted mice and decreased expression in diabetic patients with hyperglycaemia. However it should be noted that these studies have only investigated mRNA expression at a single time point and there may be a delay from altered transcription to protein. Further studies will be

required to elucidate how changes in protein levels may alter such feedback pathways. However taken together, these findings indicate that intestinal feedback mechanisms and therein, taste molecules, are dynamic and influenced by both systemic and luminal nutrient exposure.

7.2 Conclusions

The mucosa of the proximal small intestine of both mice and humans is a distinct site of expression of key molecules involved in sweet taste signalling. The regional and cell specific expression of these molecules suggests the gut is able to 'tastes' its contents in a similar way to the tongue and therefore this pathway may respresent one way that the epithelium is able to identify nutrient. It is yet to be determined precisely how this nutrient sensing mechanism operates, the mediators released and nerve pathways activated by intestinal taste cells, however these studies have shown that taste transduction in the gut is likely to be complex, and involve heterogeneous populations of primary sensor cells and multiple mediators. Furthermore this research has provided the first evidence that intestinal taste molecules are dynamically regulated by both systemic and luminal nutrient exposure. This increased understanding of taste signalling pathways in the gastrointestinal tract of mice and humans has significant implications for future therapeutic agents. It may be possible to exploit tastant-induced release of gastrointestinal neurotransmitters or to design novel drugs that target this signalling cascade in the future. Such strategies would provide a novel approach to pharmacotherapy in patients with upper gastrointestinal motility disorders and/or diabetes.